Crucial role of SLP-76 and ADAP for neutrophil recruitment in mouse kidney ischemia-reperfusion injury

Helena Block,[1,2] Jan M. Herter,[1,2] Jan Rossaint,[1,2] Anika Stadtmann,[1,2] Stefanie Kliche,[3] Clifford A. Lowell,[4] and Alexander Zarbock[1,2]

[1]Department of Anesthesiology and Critical Care Medicine, University of Münster, 48149 Münster, Germany
[2]Max-Planck Institute for Molecular Biomedicine, 48149 Münster, Germany
[3]Institute of Molecular and Clinical Immunology, Otto-von-Guericke University Magdeburg, 39120 Magdeburg, Germany
[4]Department of Laboratory Medicine, University of California, San Francisco, San Francisco, CA 94143

Neutrophils trigger inflammation–induced acute kidney injury (AKI), a frequent and potentially lethal occurrence in humans. Molecular mechanisms underlying neutrophil recruitment to sites of inflammation have proved elusive. In this study, we demonstrate that SLP-76 (SH2 domain–containing leukocyte phosphoprotein of 76 kD) and ADAP (adhesion and degranulation promoting adaptor protein) are involved in E-selectin–mediated integrin activation and slow leukocyte rolling, which promotes ischemia–reperfusion–induced AKI in mice. By using genetically engineered mice and transduced $Slp76^{-/-}$ primary leukocytes, we demonstrate that ADAP as well as two N-terminal–located tyrosines and the SH2 domain of SLP-76 are required for downstream signaling and slow leukocyte rolling. The Tec family kinase Bruton tyrosine kinase is downstream of SLP-76 and, together with ADAP, regulates PI3Kγ (phosphoinositide 3-kinase–γ)- and PLCγ2 (phospholipase Cγ2)-dependent pathways. Blocking both pathways completely abolishes integrin affinity and avidity regulation. Thus, SLP-76 and ADAP are involved in E-selectin–mediated integrin activation and neutrophil recruitment to inflamed kidneys, which may underlie the development of life-threatening ischemia-reperfusion–induced AKI in humans.

CORRESPONDENCE
Alexander Zarbock:
zarbock@uni-muenster.de

Abbreviations used: ADAP, adhesion and degranulation promoting adaptor protein; AKI, acute kidney injury; Btk, Bruton tyrosine kinase; IRI, ischemia-reperfusion injury; MAPK, mitogen-activated protein kinase; PI3K, phosphoinositide 3-kinase; PLC, phospholipase C; PTx, pertussis toxin; RIR, renal ischemia-reperfusion; shRNA, short hairpin RNA; Syk, spleen tyrosine kinase.

Efficient leukocyte recruitment is required for inflammatory responses (Ley et al., 2007). Neutrophils rapidly migrate into inflamed tissue and contribute to early inflammatory responses (Nathan, 2006; O'Shea and Murray, 2008). Their recruitment into inflamed tissue must be tightly regulated so that the number of migrated neutrophils is sufficient to control infection without injuring the surrounding tissue and leading to organ dysfunction (Serhan and Savill, 2005; Eltzschig and Carmeliet, 2011). This is demonstrated in acute inflammatory insults of the kidney, where neutrophil–mediated inflammation causes acute kidney injury (AKI; Bonventre and Weinberg, 2003; Singbartl and Ley, 2004). Ischemia-reperfusion injury (IRI) is the leading cause of AKI, which is associated with high morbidity and mortality (Thadhani et al., 1996).

Neutrophil recruitment to postischemic tissue has been identified as a hallmark of kidney injury (Bonventre and Weinberg, 2003). Neutrophil emigration into inflamed tissues proceeds in a complex sequence of events (Ley et al., 2007). The first steps of this cascade are mediated by endothelial selectins interacting with their counter receptors on leukocytes (Ley et al., 2007). During the contact of leukocytes with the inflamed endothelium, leukocytes are activated by different stimuli (Ley et al., 2007; Zarbock and Ley, 2008). This leads to integrin activation, arrest, crawling, and subsequent extravasation of leukocytes into the inflamed tissue (Ley et al., 2007).

E-selectin binding to PSGL-1 (P-selectin glycoprotein ligand-1) on neutrophils activates a signaling pathway in rolling neutrophils that cooperates with chemokine-induced signaling to amplify neutrophil recruitment during inflammation (Smith et al., 2004; Zarbock et al., 2007a).

The signaling pathway triggered by E-selectin engagement induces the activation of a receptor-proximal Src family ITAM (immunoreceptor tyrosine–based activation motif)-containing adaptor protein–Syk (spleen tyrosine kinase) signaling pathway, which induces LFA-1 (lymphocyte function–associated antigen-1)–dependent slow rolling in vitro and in vivo (Zarbock et al., 2007a, 2008; Kuwano et al., 2010; Yago et al., 2010). Src family kinase activation after E-selectin engagement (Zarbock et al., 2008; Yago et al., 2010) induces phosphorylation of the ITAM-containing adaptor proteins DAP12 (*Tyrobp*) and FcRγ (*Fcrg*). Thus, phosphorylated DAP12 and FcRγ associate and subsequently activate Syk (Zarbock et al., 2008), which is required for E-selectin–mediated slow leukocyte rolling (Zarbock et al., 2007a). E-selectin–mediated phosphorylation of DAP12 and Syk is absent in $Fgr^{-/-}$ and $Lyn^{-/-}/Hck^{-/-}$ neutrophils (Zarbock et al., 2008; Yago et al., 2010). Similarly, $Tyrobp^{-/-}/Fcrg^{-/-}$ mice display reduced Syk phosphorylation and abolished slow rolling of neutrophils upon E-selectin triggering (Zarbock et al., 2008; Yago et al., 2010). The Tec family kinase Bruton tyrosine kinase (Btk) is downstream of Syk (Mueller et al., 2010; Yago et al., 2010) and regulates two pathways (Mueller et al., 2010). One pathway is PI3Kγ (phosphoinositide 3-kinase–γ) dependent and the other pathway comprises PLCγ2 (phospholipase Cγ2), p38 mitogen-activated protein kinase (MAPK), and Rap1a (Ras-related protein 1a; Mueller et al., 2010; Stadtmann et al., 2011).

SLP-76 (SH2 domain–containing leukocyte phosphoprotein of 76 kD) is an immune cell adaptor (Jordan et al., 2003), which was originally described as a key regulator of TCR signaling events (Motto et al., 1996; Yablonski et al., 1998). SLP-76 was subsequently shown to be involved in signaling in other hematopoietic lineages, including platelets (Clements et al., 1999; Judd et al., 2000, 2002), mast cells (Kettner et al., 2003), and neutrophils (Newbrough et al., 2003). Elimination of SLP-76 abolishes integrin-mediated outside-in signaling in neutrophils (Newbrough et al., 2003) and leads to marked defects in neutrophil-dependent inflammation (Newbrough et al., 2003; Clemens et al., 2007; Lenox et al., 2009). SLP-76 consists of a C-terminal SH2 domain, a proline-rich region, a sterile α motif domain, and an N-terminal acidic domain containing three tyrosines at positions 112, 128, and 145. These tyrosines are phosphorylated upon immunoreceptor and integrin engagement (Bubeck Wardenburg et al., 1996; Fang et al., 1996; Jordan et al., 2006), and SH2 domain–containing proteins such as the guanine nucleotide exchange factor Vav (Y112 and Y128; Raab et al., 1997; Gross et al., 1999), the adaptor noncatalytic region of tyrosine kinase Nck (Y112 and Y128), and Btk (Y145) have been identified as interaction partners of these tyrosines (Bubeck Wardenburg et al., 1998; Su et al., 1999). The C-terminal SH2 domain of SLP-76 is associated with the immune cell adaptor ADAP (adhesion and degranulation promoting adaptor protein; Raab et al., 1997; Myung et al., 2001).

ADAP is expressed in various hematopoietic cell types, including neutrophils. This protein consists of an EVH1

(Ena/VASP homology 1) binding domain, two helical SH3-like domains, several tyrosine-based signaling motifs, and a central proline-rich region (Krause et al., 2000; Heuer et al., 2005). Experiments in ADAP-deficient mice revealed a role of this adaptor protein in TCR-mediated activation of the integrin LFA-1. ADAP-deficient T cells show defective TCR-mediated adhesion and LFA-1 clustering (Griffiths et al., 2001; Peterson et al., 2001). TCR-mediated phosphorylation of ADAP at the tyrosine-based signaling motifs YDDV through the Src kinase Fyn mediates the inducible interaction with the SH2 domain of SLP-76 (da Silva et al., 1997; Musci et al., 1997; Geng et al., 1999; Raab et al., 1999; Veale et al., 1999). Mutation of these YDDV sites of ADAP disrupts TCR-induced adhesion and LFA-1 clustering, indicating that the inducible interaction between ADAP and SLP-76 is required for LFA-1 activation (Wang et al., 2004). Furthermore, ADAP is also involved in adhesion processes of platelets and basophilic cells (Geng et al., 2001; Kasirer-Friede et al., 2007). However, the functional role of ADAP and SLP-76 in neutrophil recruitment has not been investigated so far.

In this study, we specifically address the role of SLP-76 and ADAP in neutrophil-mediated inflammation in mice. We show that the presence of SLP-76 and ADAP is required for E-selectin–mediated slow leukocyte rolling and leukocyte recruitment. Experiments with knockin mice demonstrate that the two tyrosines Y112 and Y128 of SLP-76 are required for slow leukocyte rolling and leukocyte recruitment into inflamed tissue. Moreover, both adaptors modulate neutrophil recruitment by regulating integrin affinity and avidity, which has a potential impact on the outcome of acute inflammatory processes.

RESULTS

Deficiency in ADAP or SLP–76 attenuates neutrophil recruitment and protects mice from AKI

To test whether SLP-76 and ADAP are involved in neutrophil recruitment and tissue damage in the context of AKI, we used a renal ischemia-reperfusion (RIR) model in chimeric mice reconstituted with BM from $Slp76^{-/-}$, $Slp76^{Y145}$ (SM), $Slp76^{Y112/128}$ (DM), $ADAP^{-/-}$, and WT control mice. After bilateral renal pedicle clamping for 32 min followed by reperfusion, WT mice and $Slp76^{Y145}$ mice showed an elevated number of neutrophils in the kidney compared with sham operated mice 24 h after reperfusion (Fig. 1 A). Concomitant with the neutrophil influx, WT and $Slp76^{Y145}$ mice that had undergone 32-min ischemia and reperfusion showed an increase in creatinine concentration 24 h after reperfusion (Fig. 1 B). $Slp76^{-/-}$, $Slp76^{Y112/128}$, and $ADAP^{-/-}$ mice had a significantly reduced number of neutrophils in the kidney (Fig. 1 A) and a lower serum creatinine concentration (Fig. 1 B) compared with WT mice when challenged with 32 min of ischemia followed by 24 h of reperfusion. RIR produced great morphological damages in kidneys from WT mice, including cell recruitment, massive tubular edema, and loss of tubular epithelial cells (Fig. 1 C). $Slp76^{-/-}$, $Slp76^{Y112/128}$,
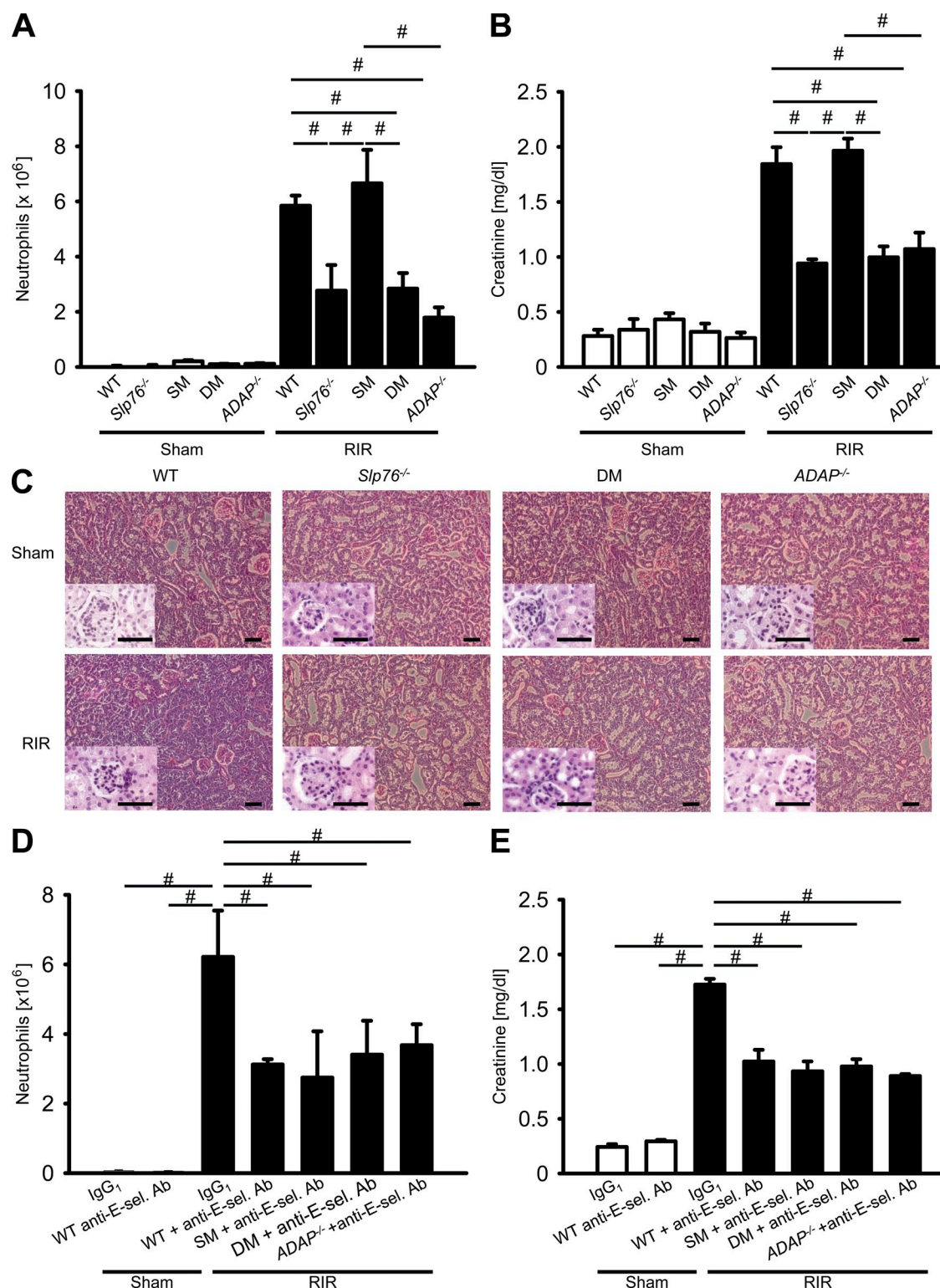
Figure 1. Deficiency in ADAP or SLP–76 attenuates neutrophil recruitment and protects mice from AKI. (A and B) Irradiated WT mice were reconstituted with BM from WT ($n = 4$), $Slp76^{-/-}$ ($n = 4$), Slp76[Y112/128] (DM; $n = 4$), Slp76[Y145] (SM; $n = 4$), and $ADAP^{-/-}$ mice ($n = 4$). 6–8 wk later, mice were subjected to RIR or sham injury, and the number of neutrophils recruited into the kidney (A) and plasma creatinine were assessed 24 h later (B). (C) Representative H&E staining of kidney outer medulla from chimeric mice was assessed 24 h after sham operation or renal IRI. Insets show a twofold magnified image. Bars, 50 µm. (D and E) Chimeric mice were pretreated with an IgG control antibody or a blocking anti–E-selectin antibody (Ab) 10 min after sham or renal IRI. 24 h later, the number of neutrophils in the kidney (D) and creatinine levels in the plasma (E) were determined. Results are presented as mean ± SEM. #, $P < 0.05$.

and *ADAP*^{-/-} mice revealed medulla hyperemia but reduced cell recruitment and cellular destruction (Fig. 1 C).

To provide more mechanistic details of downstream signaling events in AKI, we investigated the phosphorylation of p38 MAPK, a molecule which is involved in the E-selectin–mediated signaling pathway, in neutrophils from control kidneys and injured kidneys. WT, *Slp76*^{-/-}, and *ADAP*^{-/-} neutrophils from control kidneys showed a similar degree of p38 MAPK phosphorylation (not depicted). After IRI, the phosphorylation of p38 MAPK was significantly reduced in *Slp76*^{-/-} and *ADAP*^{-/-} neutrophils compared with WT neutrophils (not depicted).

Application of a blocking E-selectin antibody (9A9) in WT and *Slp76*[Y145] mice 10 min after reperfusion significantly decreased the number of neutrophils in the kidney (Fig. 1 D) and reduced the creatinine concentration in the plasma

(Fig. 1 E) compared with WT mice that had undergone ischemia and reperfusion and had been treated with a matched isotype control antibody (Fig. 1, D and E). These data suggest that E-selectin promotes neutrophil recruitment to sites of inflammation, which increases tissue damage in inflamed kidneys. Injecting a blocking E-selectin antibody in *Slp76*[Y112/128] and *ADAP*^{-/-} mice did not further decrease the number of neutrophils in the kidney (Fig. 1 D) and creatinine concentration (Fig. 1 E) 24 h after IRI, suggesting that ADAP and SLP-76 are crucially involved in E-selectin–mediated neutrophil recruitment.

SLP–76 and ADAP are involved in controlling leukocyte rolling velocity and adhesion after IRI

To directly visualize leukocyte rolling and adhesion in the kidney, we performed intravital microscopy of the kidney before and after inducing ischemia-reperfusion–induced AKI. After sham operation, almost no rolling and adherent leukocytes were observed (not depicted). 4 h after renal IRI, leukocyte rolling velocity in LysM-GFP mice was 8.7 ± 1.3 µm/s in small vessels in the cortex of the kidney (Fig. 2 A). Blocking of Mac-1 by an antibody did not elevate the rolling velocity,
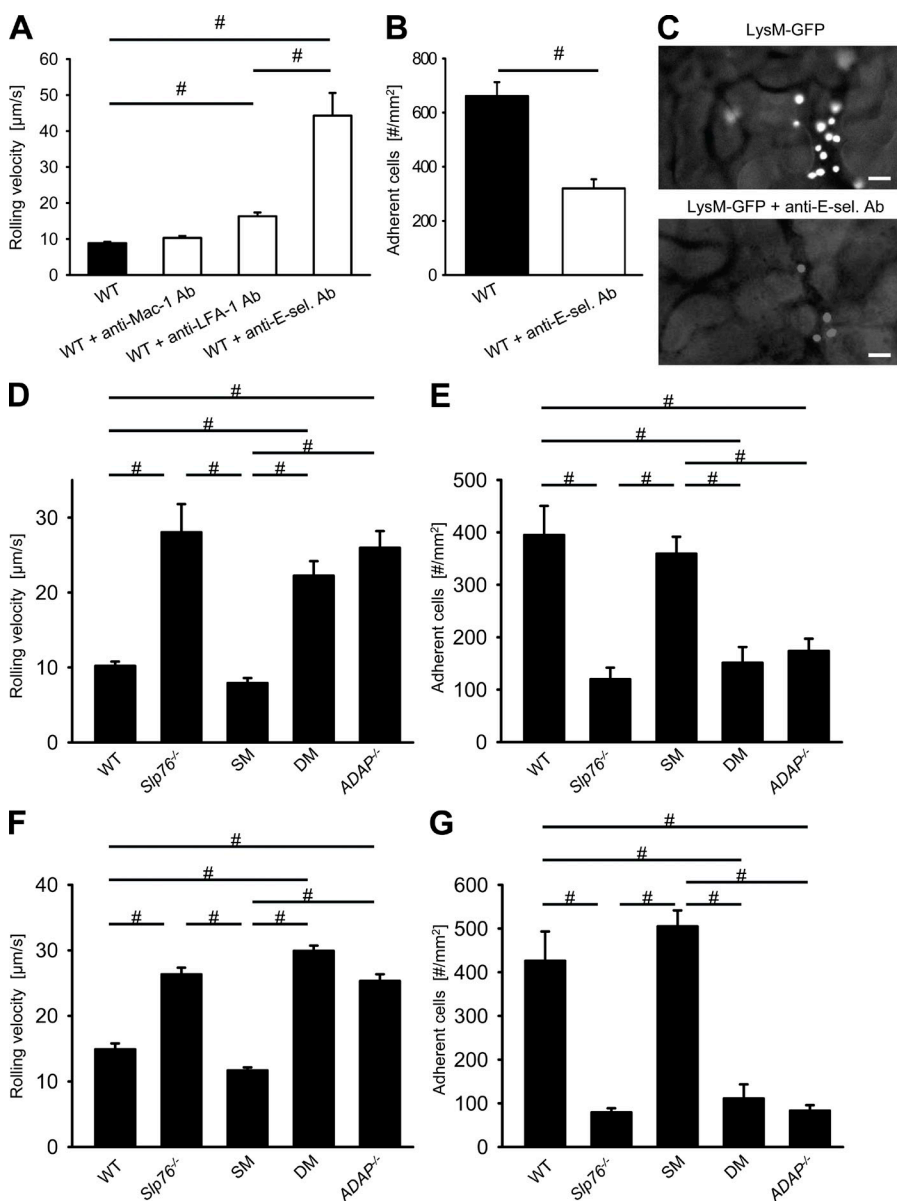

Figure 2. Leukocyte rolling and adhesion in kidney or cremaster venules after ischemia–reperfusion is dependent on SLP–76 and ADAP. (A and B) Untreated LysM-GFP mice or LysM-GFP mice pretreated with different antibodies (anti–Mac-1 antibody [M1-70], $n = 3$; anti-LFA-1 antibody [TIB217], $n = 3$; and anti–E-selectin antibody [9A9], $n = 3$) were subjected to RIR, and the rolling velocity (A) and the number of adherent leukocytes (B) in venules of the kidney were determined. (C) Representative pictures of cremaster muscle postcapillary venules of untreated LysM-GFP mice and LysM-GFP mice pretreated with a blocking anti–E-selectin antibody (Ab) 4 h after renal IRI. Bars, 25 µm. (D and E) 2 h after RIR, WT mice were injected i.v. with fluorescently labeled BM cells from WT ($n = 3$), Slp76^{-/-} ($n = 3$), *Slp76*[Y145] (SM; $n = 3$), *Slp76*[Y112/128] (DM; $n = 3$) or *ADAP*^{-/-} ($n = 3$) mice. 2 h later, leukocyte rolling velocity (D) and the number of adherent cells (E) in venules of the kidney were determined. (F and G) The cremaster muscle of WT ($n = 3$), Slp76^{-/-} ($n = 3$), *Slp76*[Y145] ($n = 3$), *Slp76*[Y112/128] ($n = 3$), and *ADAP*^{-/-} ($n = 3$) mice was subjected to ischemia (30 min)/reperfusion (120 min) injury, and mean rolling velocity (F) and the number of adherent cells (G) in postcapillary venules of the cremaster muscle were determined. Results are presented as means $\pm$ SEM. #, P < 0.05.

whereas blocking of LFA–1 significantly elevated the rolling velocity (Fig. 2 A). Blocking E-selectin by a blocking monoclonal anti–E-selectin antibody significantly elevated the rolling velocity of leukocytes and also reduced the number of adherent leukocytes compared with untreated WT mice (Fig. 2, A and B). Representative video micrographs of WT mice and WT mice treated with a monoclonal antibody to E-selectin 4 h after renal IRI are shown in Fig. 2 C.

To directly investigate the contributions of ADAP and SLP-76 to slow rolling and adhesion in the kidney, we labeled WT, $ADAP^{-/-}$, $Slp76^{-/-}$, SM, or DM leukocytes with a fluorescent dye and injected the labeled leukocytes i.v. into recipient WT mice 2 h after inducing renal IRI. Compared with WT leukocytes, SM leukocytes showed the same rolling velocity and adhesion characteristics (Fig. 2, D and E). $Slp76^{-/-}$, DM, and $ADAP^{-/-}$ leukocytes had an elevated rolling velocity and reduced leukocyte adhesion compared with WT leukocytes (Fig. 2, D and E). Shear rates and diameters were similar between different groups, excluding a hemodynamic contribution to reduced leukocyte rolling velocity and adhesion (not depicted). These data demonstrate that the protection from renal IRI is caused by decreased E-selectin–mediated slow leukocyte rolling and adhesion.

To confirm our data, we conducted intravital microscopy of the cremaster muscle before and after IRI. Compared with WT mice, $Slp76^{-/-}$, $ADAP^{-/-}$, SM, and DM mice showed the same leukocyte rolling velocity and number of adherent leukocytes before inducing IRI (not depicted). SM mice showed the same leukocyte rolling velocity and a similar number of adherent leukocytes after IRI compared with WT mice (Fig. 2, F and G). $Slp76^{-/-}$, DM, and $ADAP^{-/-}$ mice had an elevated leukocyte rolling velocity and reduced number of adherent leukocytes compared with WT mice after IRI (Fig. 2, F and G). Shear rates and diameters were similar between different groups, excluding a hemodynamic contribution to reduced leukocyte adhesion (not depicted). These data demonstrate that ADAP and SLP-76 are involved in the regulation of the leukocyte rolling velocity after IRI.

SLP–76 and ADAP are required for E-selectin–mediated slow leukocyte rolling and $G\alpha_i$-independent adhesion

To test whether SLP-76 and ADAP are involved in E-selectin–mediated slow rolling, we investigated the rolling velocity of neutrophils from $Slp76^{-/-}$, SM, DM, $ADAP^{-/-}$, and WT mice in an autoperfused flow chamber. We have previously shown that the rolling velocity of WT neutrophils rolling on E-selectin– and ICAM-1 (intercellular adhesion molecule-1)–coated autoperfused flow chambers is significantly reduced compared with E-selectin alone (Zarbock et al., 2007a, 2008; Mueller et al., 2010). Neutrophils from $Slp76^{-/-}$, DM, and $ADAP^{-/-}$ mice showed a similar rolling velocity on E-selectin compared with WT neutrophils but failed to reduce their rolling velocity on E-selectin plus ICAM-1 (Fig. 3, A–C). In contrast, SM neutrophils showed the same rolling velocity on E-selectin and ICAM-1 compared with WT neutrophils (Fig. 3 B). To support our flow chamber data, we conducted

intravital microscopy of the cremaster muscle in mixed chimeric mice generated by injecting BM cells from WT LysM-GFP$^+$ mice (Faust et al., 2000) and $Slp76^{-/-}$ mice or $ADAP^{-/-}$ mice (GFP$^-$) into lethally irradiated WT mice. Leukocyte rolling velocity was analyzed in TNF-induced inflamed venules of the cremaster muscle after blocking P-selectin and $G\alpha_i$ signaling to focus on E-selectin–mediated slow rolling (Zarbock et al., 2007a). The mean blood flow velocity and the wall shear rates in these venules were 2.5 ± 0.3 mm/s and 2,000 ± 200 s^{-1}, respectively. The mean rolling velocity (V_{avg}) of $Slp76^{-/-}$, DM, and $ADAP^{-/-}$ leukocytes was significantly elevated compared with the mean rolling velocity of LysM-GFP$^+$ control and SM leukocytes (Fig. 3, D–F). The rolling velocity of $Slp76^{-/-}$, DM, and $ADAP^{-/-}$ leukocytes is similar to the rolling velocity of leukocytes seen in WT mice after blocking LFA-1, the integrin responsible for slow leukocyte rolling (Zarbock et al., 2007a).

Firm adhesion of leukocytes in the postcapillary venules of the cremaster muscle after TNF application is mediated in an overlapping fashion by E-selectin and $G\alpha_i$ signaling (Mueller et al., 2010). WT, $Slp76^{-/-}$, DM, and $ADAP^{-/-}$ mice showed the same number of adherent cells 2 h after TNF application. Pretreatment of WT or SM mice with pertussis toxin (PTx) did not affect the number of adherent cells, whereas blocking of $G\alpha_i$ signaling by PTx significantly reduced the number of adherent cells in $Slp76^{-/-}$, DM, and $ADAP^{-/-}$ mice (Fig. 3, G–I). These findings suggest that SLP-76 is involved in LFA-1 activation and subsequently in slow rolling in response to E-selectin engagement. Hemodynamic and microvascular parameters were equivalent in venules of all genotypes (not depicted).

To test whether SLP-76 and ADAP are involved in chemokine-induced arrest, we conducted intravital microscopy of the untreated cremaster muscle (Zarbock et al., 2007a). In this model, neutrophils roll in cremaster venules because of P-selectin expression on the endothelium but rarely adhere. Injection of 600 ng of recombinant murine CXCL1, which binds CXCR2, induced the same number of adherent leukocytes in venules of chimeric mice reconstituted with BM from WT, $Slp76^{-/-}$, or $ADAP^{-/-}$ mice (450 ± 60 adherent cells/mm^2, 470 ± 21 adherent cells/mm^2, and 451 ± 46 adherent cells/mm^2, respectively). These data suggest that SLP-76 and ADAP are required for E-selectin–mediated slow rolling but are not involved in chemokine-induced leukocyte arrest.

It has been shown that the arginine at position 448 in SLP-76 is important for the interaction with ADAP (Musci et al., 1997). To investigate its contribution in E-selectin–mediated slow rolling, we conducted reconstitution experiments. SLP-76–deficient cells were reconstituted with a WT construct of SLP-76, a Slp76R448K mutant construct (mutation of the arginine at position 448), or the empty vector. The WT construct could compensate SLP-76 deficiency, whereas the Slp76R448K mutant construct and the empty vector failed to restore slow leukocyte rolling in TNF-induced inflamed postcapillary venules of the cremaster muscle after
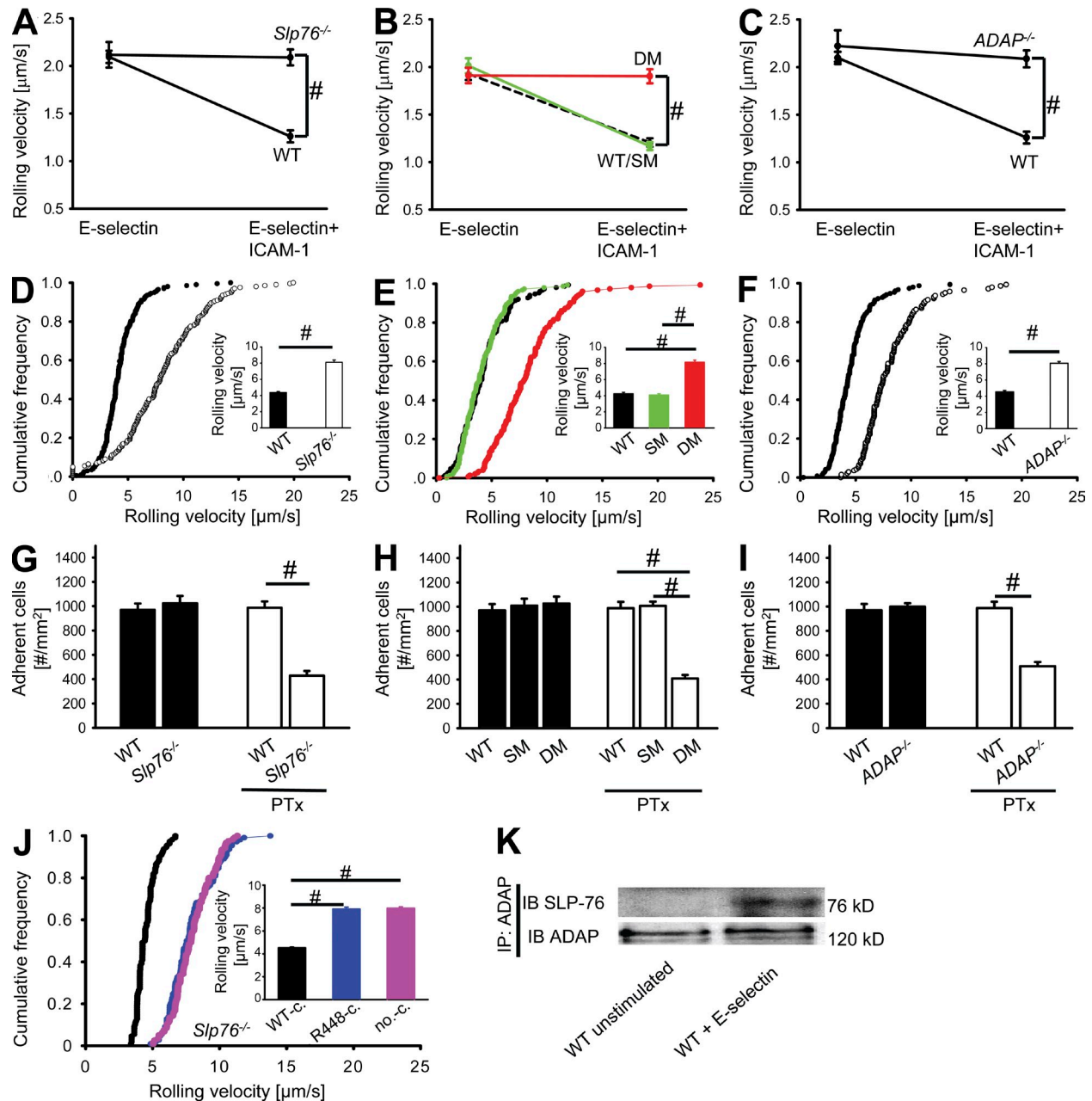
Figure 3. SLP–76 tyrosines are required for E-selectin–mediated slow leukocyte rolling and Gαᵢ–independent adhesion. (A–C) The carotid artery of chimeric mice reconstituted with BM from WT ($n = 3$) or $Slp76^{-/-}$ ($n = 3$) mice (A), with WT ($n = 3$), SM ($n = 3$), or DM ($n = 3$) mice (B), or with WT ($n = 3$) or ADAP ($n = 3$) mice (C) was cannulated with a catheter, which was connected to autoperfused flow chambers. Mean rolling velocity of neutrophils on E-selectin (left) and E-selectin and ICAM-1 (right) is presented as means ± SEM. The wall shear stress in all flow chamber experiments was 5–6 dyn/cm². #, P < 0.05. (D–F) Mixed chimeric mice were generated by injecting BM cells from LysM-GFP⁺ WT (WT; D–F) mice and $Slp76^{-/-}$ ($Slp76^{-/-}$; D), SM (E) and DM mice (E), or ADAP⁻/⁻ mice ($ADAP^{-/-}$; F) into lethally irradiated WT mice. Cumulative histogram of rolling velocities of 100 GFP⁺ (WT) and 100 GFP⁻ leukocytes in inflamed cremaster muscle venules of mixed chimeric mice ($n = 4$) treated with PTx and a monoclonal blocking P-selectin antibody (RB40.34). The insets show the mean rolling velocity ± SEM. #, P < 0.05. (G–I) Numbers of adherent cells per square millimeter in murine cremaster muscle venules. The cremaster muscle was exteriorized 2 h after intrascrotal injection of 500 ng TNF or after injection of TNF and PTx in chimeric mice reconstituted with BM from WT mice (G–I; $n = 3$) or $Slp76^{-/-}$ (G; $n = 3$), SM and DM (H), or $ADAP^{-/-}$ (I) mice. Results are presented as means ± SEM. #, P < 0.05. (J) Mixed chimeric mice were generated by injecting retrovirally transduced hematopoietic stem cells (Slp-76–WT construct, WT-c.; Slp76-R448K construct, R448-c.; empty vector, no-c.) from $Slp76^{-/-}$ mice into lethally irradiated WT mice. Cumulative histogram of rolling velocities of transduced (WT-c., $n = 100$; R448-c., $n = 100$; no-c., $n = 100$) leukocytes in inflamed cremaster muscle venules of mixed chimeric mice ($n = 3$) treated with PTx and a monoclonal blocking P-selectin antibody. The inset shows the mean rolling velocity ± SEM. #, P < 0.05. (K) Coimmunoprecipitation of SLP-76 and ADAP. BM-derived WT neutrophils were plated on uncoated (unstimulated) or E-selectin–coated wells for 10 min, and then lysates were prepared followed by immunoprecipitation (IP) with ADAP antibody. Precipitates were immunoblotted (IB) with antibodies to total SLP-76 (top) and total ADAP (bottom).

blocking P-selectin and $G\alpha_i$ signaling (Fig. 3 J). Microvascular parameters (vessel diameters, centerline velocities, and wall shear rates) were similar among the groups (not depicted). In addition to these data, coimmunoprecipitation experiments suggest that SLP-76 and ADAP physically interact after E-selectin engagement (Fig. 3 K). These findings suggest that the two tyrosines Y112 and Y128 of SLP-76 and the interaction between SLP-76 and ADAP are required for LFA-1 activation and subsequent slow leukocyte rolling after E-selectin engagement.

The presence of SLP-76 and ADAP is required for E-selectin–mediated LFA-1 affinity and avidity regulation

E-selectin engagement mediates LFA-1 activation, which is accompanied by a shape change to the extended conformation (Kuwano et al., 2010). To directly investigate the role of different signaling molecules in selectin-mediated integrin activation, we used an immobilized reporter antibody assay, which provides a robust readout of the extended conformation of LFA-1 (Kuwano et al., 2010). As this antibody is only available for human cells, we performed short hairpin RNA (shRNA) experiments in which we transfected the promyelocytic cell line HL-60 with shRNA constructs against SLP-76 or ADAP (Horn et al., 2009). Down-regulation of SLP-76 and ADAP was confirmed by Western blot analysis (Fig. 4, A and B). These experiments revealed that the number of adherent cells per field of view (Fig. 4 C) was significantly reduced when the expression of SLP-76 or ADAP was down-regulated, indicating that the affinity of LFA-1 is reduced in the absence of these molecules.

By using pharmacological inhibitors against Btk, PLC, and PI3Kγ, we were able to investigate the role of these molecules in E-selectin–mediated regulation of LFA-1 affinity (Fig. 4 D). In this study, we observed that blocking PLC or PI3Kγ partially, but significantly, inhibited the number of adherent cells on the reporter antibody KIM127 after E-selectin engagement (Fig. 4 D). Inhibiting both molecules, PLC and PI3Kγ, or Btk led to an even stronger reduction of adherent cells in this setting (Fig. 4 D). These findings suggest that E-selectin engagement controls LFA-1 function via its affinity and that PLCγ2- and PI3Kγ-dependent pathways control the regulation of LFA-1 conformation.

Another well-described aspect of integrin activation is its clustering on the cell surface. To investigate LFA-1 clustering, we performed intravital microscopy of the cremaster muscle after pretreating the mice with TNF and a blocking antibody against P-selectin and visualized LFA-1 clustering by staining leukocytes with a fluorescently labeled antibody against LFA-1. Clustering of surface adhesion molecules was determined as described previously (Stadtmann et al., 2011), and the percentage of rolling leukocytes with clustered LFA-1 was calculated. In WT mice, LFA-1 clustered on one edge of rolling leukocytes. Furthermore, we showed that >80% of WT leukocytes display LFA-1 clustering (Fig. 4 E), whereas $Slp76^{Y112/128}$, $Btk^{-/-}$, and $ADAP^{-/-}$ leukocytes show a strong reduction of LFA-1 clustering (Fig. 4 E).

However, $Pik3cg^{-/-}$ and $Plcg2^{-/-}$ leukocytes showed a significantly elevated LFA-1 clustering frequency compared with $Slp76^{Y112/128}$, $Btk^{-/-}$, and $ADAP^{-/-}$ leukocytes (Fig. 4 E). Representative video micrographs of WT leukocytes and $Btk^{-/-}$ leukocytes during E-selectin–mediated slow leukocyte rolling are shown in Fig. 4 F.

$G\alpha_i$–independent leukocyte extravasation and neutrophil recruitment are defective in $Slp76^{-/-}$, $Slp76^{Y112/128}$, and $ADAP^{-/-}$ mice

Leukocyte extravasation in the cremaster muscle after TNF application and neutrophil recruitment into the inflamed peritoneal cavity is promoted by E-selectin– and $G\alpha_i$–dependent pathways (Mueller et al., 2010). To investigate the contribution of SLP-76 and ADAP on the number of transmigrated leukocytes, we visualized extravasated leukocytes in the cremaster muscle using reflected-light oblique transillumination microscopy (Mueller et al., 2010). Chimeric mice reconstituted with BM from WT mice or $Slp76^{Y145}$ mice treated with 4 µg PTx via tail vein injection before intrascrotal injection of 500 ng TNF showed no reduction in leukocyte extravasation versus chimeric mice reconstituted with BM from WT or $Slp76^{Y145}$ mice that did not receive PTx treatment (Fig. 5 A). In chimeric mice reconstituted with BM from $Slp76^{-/-}$, $Slp76^{Y145}$, $Slp76^{Y112/128}$, and $ADAP^{-/-}$ mice, the number of extravasated leukocytes was similar to that observed in WT mice (Fig. 5 A). However, pretreating chimeric mice reconstituted with BM from $Slp76^{-/-}$, $Slp76^{Y112/128}$, and $ADAP^{-/-}$ mice with PTx almost completely abolished leukocyte extravasation (Fig. 5 A). These data suggest that the E-selectin–mediated signaling pathway leading to integrin activation is defective in $Slp76^{-/-}$, $Slp76^{Y112/128}$, and $ADAP^{-/-}$ leukocytes.

Neutrophil recruitment in thioglycollate-induced peritonitis was also investigated in chimeric mice reconstituted with BM from WT, $Slp76^{-/-}$, $Slp76^{Y112/128}$, and $ADAP^{-/-}$ mice with or without PTx treatment to block $G\alpha_i$ signaling. In the presence of intact GPCR (G protein–coupled receptor) signaling, chimeric mice reconstituted with BM from $Slp76^{-/-}$, $Slp76^{Y112/128}$, and $ADAP^{-/-}$ mice showed a normal number of neutrophils in the peritoneal cavity 8 h after thioglycollate injection (Fig. 5 B). Pretreating chimeric mice reconstituted with BM from WT mice with PTx diminished neutrophil recruitment into the peritoneal cavity by ~50%. However, blocking of $G\alpha_i$ signaling by PTx in chimeric mice reconstituted with BM from $Slp76^{-/-}$, $Slp76^{Y112/128}$, and $ADAP^{-/-}$ mice completely abolished neutrophil recruitment into the peritoneal cavity after thioglycollate injection (Fig. 5 B).

SLP-76 and ADAP are required for downstream signaling after E-selectin engagement

To investigate how SLP-76 and ADAP are integrated in the E-selectin–mediated signaling pathway leading to integrin activation, we used a previously published in vitro selectin engagement assay (Zarbock et al., 2008; Mueller et al., 2010).
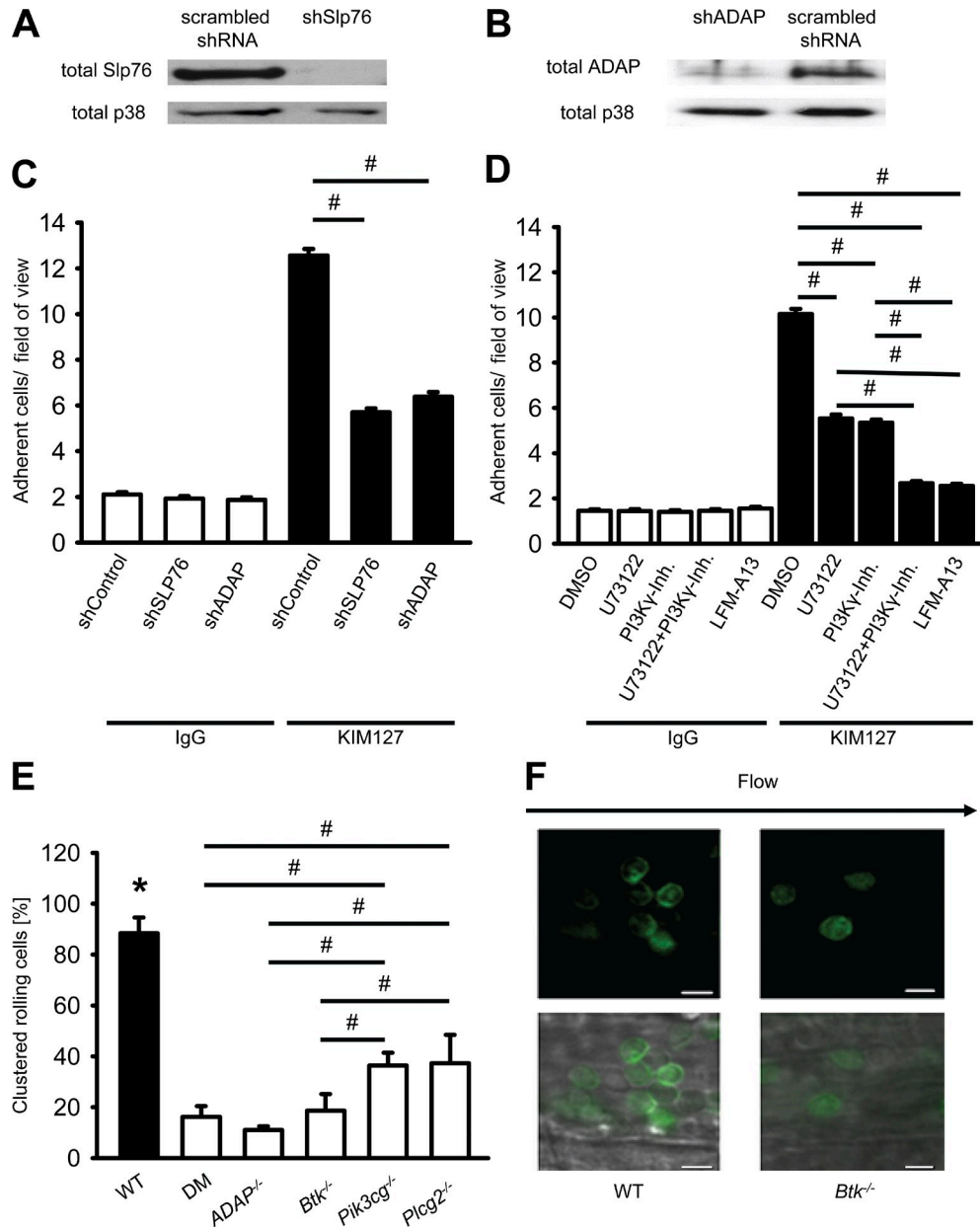
Figure 4. E–selectin modulates integrin adhesiveness by regulating integrin affinity and avidity. (A and B) HL-60 cells were transfected with control shRNA or with shRNAs against SLP-76 or ADAP and subjected to immunoblot to verify down-regulation of SLP-76 (A) and ADAP down-regulation (B). Total p38 MAPK expression was used as loading control. (C) HL-60 cells were transfected with control shRNA or with shRNAs against SLP-76 or ADAP and were used in a flow chamber adhesion assay. Flow chambers were coated with E-selectin and a control IgG antibody (open bars) or KIM127 antibody, recognizing the intermediate affinity conformation of LFA-1 (closed bars) and perfused with transfected HL-60 cells. Bars represent the number of adherent cells per field of view as mean ± SEM of three independent experiments. #, P < 0.05. (D) Flow chamber adhesion assay with human leukocytes in whole blood pretreated with DMSO or specific inhibitors against PLC (U73122), PI3Kγ, or Btk (LFM-A13). Flow chambers were coated with E-selectin and a control IgG antibody (open bars) or KIM127 antibody (closed bars). Bars show the number of adherent cells per field of view as mean ± SEM of three independent experiments. #, P < 0.05. (E) Chimeric mice reconstituted with BM from WT, Slp76$^{Y112/128}$, ADAP$^{-/-}$, Btk$^{-/-}$, Pik3cg$^{-/-}$, or Plcg2$^{-/-}$ mice were used to investigate LFA-1 clustering on rolling cells in vivo. Mice were pretreated with TNF and PTx 2 h before the experiments, and a blocking P-selectin antibody and an Alexa Fluor–conjugated LFA-1 antibody were injected immediately before preparing the cremaster muscle for intravital microscopy analysis. Cells were classified as clustered if fluorescence was >1.5 times increased at one edge of the cell. Data are shown as percentage of clustered cells as mean ± SEM of three independent measurements with at least 100 cells per group. #, P < 0.05; *, P < 0.05 versus other groups. (F) Representative images of rolling leukocytes in inflamed cremaster venules of WT and Btk$^{-/-}$ mice stained for LFA-1 clustering. Bars, 10 µm.

Stimulation of WT neutrophils with E-selectin under shear stress conditions induced phosphorylation of SLP-76 (Fig. 6, A and B), ADAP (Fig. 6, E and F), Syk (Fig. 6, C and G), Btk (Fig. 6, C, D, G, and H), PLCγ2 (Tyr1217), Akt as a target of PI3K, and p38 MAPK (Fig. 6, C, D, G, and H). To demonstrate that SLP-76 and ADAP are downstream of DAP12 and FcRγ, *Tyrobp*⁻/⁻*Fcrg*⁻/⁻ neutrophils were stimulated with E-selectin under shear stress conditions. In *Tyrobp*⁻/⁻*Fcrg*⁻/⁻ neutrophils, phosphorylation of SLP-76 (Fig. 6 A) and ADAP (Fig. 6 E) was absent, but phosphorylation of SLP-76 and ADAP in *Btk*⁻/⁻ neutrophils was present (Fig. 6, B and F). After E-selectin engagement, Syk phosphorylation was present in *Slp76*⁻/⁻ (Fig. 6 C) and in *ADAP*⁻/⁻ neutrophils (Fig. 6 G). In *Slp76*⁻/⁻ neutrophils, phosphorylation of Btk was absent (Fig. 6 C), whereas Btk phosphorylation was present in *ADAP*⁻/⁻ neutrophils (Fig. 6 G) after E-selectin engagement. In *Slp76*⁻/⁻ and *ADAP*⁻/⁻ neutrophils, phosphorylation of PLCγ2 (Tyr1217), Akt, and p38 MAPK was abolished (Fig. 6, C and G). These findings show that SLP-76 and ADAP are required for the activation of the PLCγ2- and PI3Kγ-dependent pathway.

To confirm the in vivo results, we also addressed the phosphorylation status of Btk, PLCγ2, PI3Kγ, and p38 MAPK in *Slp76*^Y112/128 mice. Similar to *Slp76*⁻/⁻ deficiency, *Slp76*^Y112/128 neutrophils displayed impaired phosphorylation of Btk, PLCγ2 (Tyr1217), Akt, and p38 MAPK in response to E-selectin stimulation (Fig. 6 D). In contrast, phosphorylation of Btk, PLCγ2 (Tyr1217), Akt, and p38 MAPK was detectable in *Slp76*^Y145 neutrophils after stimulation with E-selectin (Fig. 6 H).

DISCUSSION

The degree of inflammation and associated organ damage is a result of complex pro- and antiinflammatory responses (Serhan and Savill, 2005; Nathan, 2006; Ley et al., 2007). As demonstrated herein for AKI, this includes regulation of neutrophil recruitment into the inflamed tissue. Neutrophil recruitment is governed by different pro- and antiinflammatory cues (Ley et al., 2007). Several studies have shown that selectin binding to their receptors on neutrophils activates Src family kinases (Wang et al., 2007; Zarbock et al., 2008; Yago et al., 2010) and induces phosphorylation of several signaling molecules (Urzainqui et al., 2002; Zarbock et al., 2008; Kuwano et al., 2010; Mueller et al., 2010; Yago et al., 2010; Stadtmann et al., 2011), integrin activation (Miner et al., 2008; Zarbock et al., 2008; Kuwano et al., 2010; Mueller et al., 2010; Yago et al., 2010; Stadtmann et al., 2011), slow rolling (Miner et al., 2008; Zarbock et al., 2008; Kuwano et al., 2010; Mueller et al., 2010; Yago et al., 2010; Stadtmann et al., 2011), and adhesion (Simon et al., 2000; Mueller et al., 2010). In this study, we demonstrated that SLP-76 and ADAP are required for selectin-mediated integrin activation and slow leukocyte rolling, which promotes ischemia-reperfusion–induced AKI in mice. Eliminating SLP-76 or ADAP blocked E-selectin–mediated signaling (unpublished data), and Gαᵢ-independent neutrophil recruitment into the peritoneal cavity was defective in *Slp76*⁻/⁻ and *ADAP*⁻/⁻ mice, confirming the physiological relevance of this signaling pathway. Furthermore, structure–function analysis of SLP-76 revealed that the two N-terminal tyrosines Y112 and Y128 and the interaction of the SH2 domain of SLP-76 with ADAP are required for downstream signaling and integrin activation.
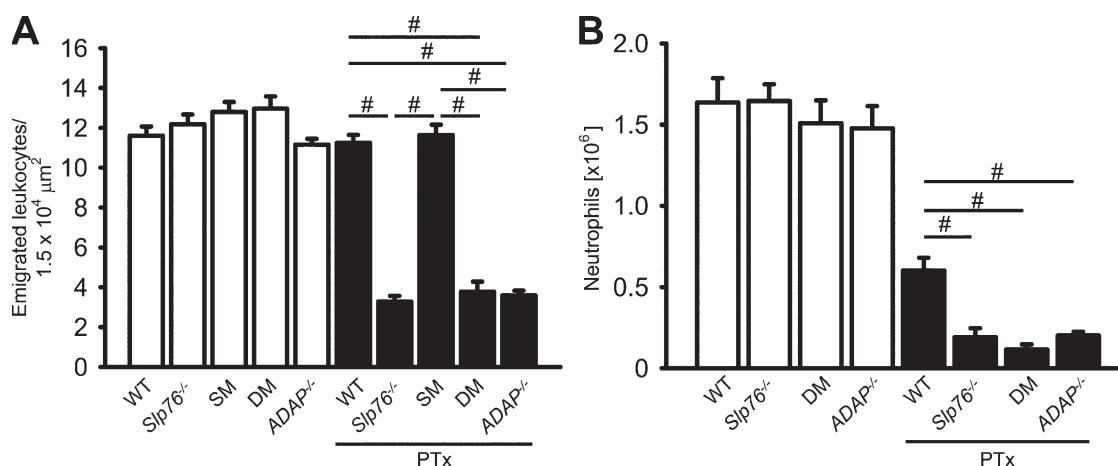

Figure 5. Gαᵢ–independent leukocyte extravasation and neutrophil recruitment is defective in *Slp76*⁻/⁻, Slp76^Y112/128, and *ADAP*⁻/⁻ mice. (A) Numbers of extravasated leukocytes in cremasteric venules of TNF–treated chimeric mice reconstituted with BM from WT (*n* = 4), *Slp76*⁻/⁻ (*n* = 4), Slp76^Y145 (SM; *n* = 4), Slp76^Y112/128 (DM; *n* = 4), or *ADAP*⁻/⁻ mice (*n* = 4) per 1.5 × 10⁴–μm² tissue area. The measurements were performed 2 h after intrascrotal TNF injection. The same groups were also analyzed after pretreatment with 4 μg PTx i.v. (+PTx; WT mice + PTx, *n* = 4; *Slp76*⁻/⁻ mice + PTx, *n* = 4; Slp76^Y145 mice + PTx, *n* = 4; Slp76^Y112/128 mice + PTx, *n* = 4; and *ADAP*⁻/⁻ mice + PTx, *n* = 4). (B) Neutrophil influx into the peritoneal cavity 8 h after 1-ml injection of 3% thioglycollate into chimeric mice reconstituted with BM from WT (*n* = 5), *Slp76*⁻/⁻ (*n* = 4), Slp76^Y112/128 (*n* = 4), or *ADAP*⁻/⁻ mice (*n* = 4). The same groups were also analyzed after pretreatment with 4 μg PTx i.v. (WT mice + PTx, *n* = 4; *Slp76*⁻/⁻ mice + PTx, *n* = 4; Slp76^Y112/128 mice + PTx, *n* = 4; and *ADAP*⁻/⁻ mice + PTx, *n* = 4). Total numbers of neutrophils in the peritoneal lavage fluid were determined by flow cytometry and hemocytometer count. Results are presented as means ± SEM. #, P < 0.05.
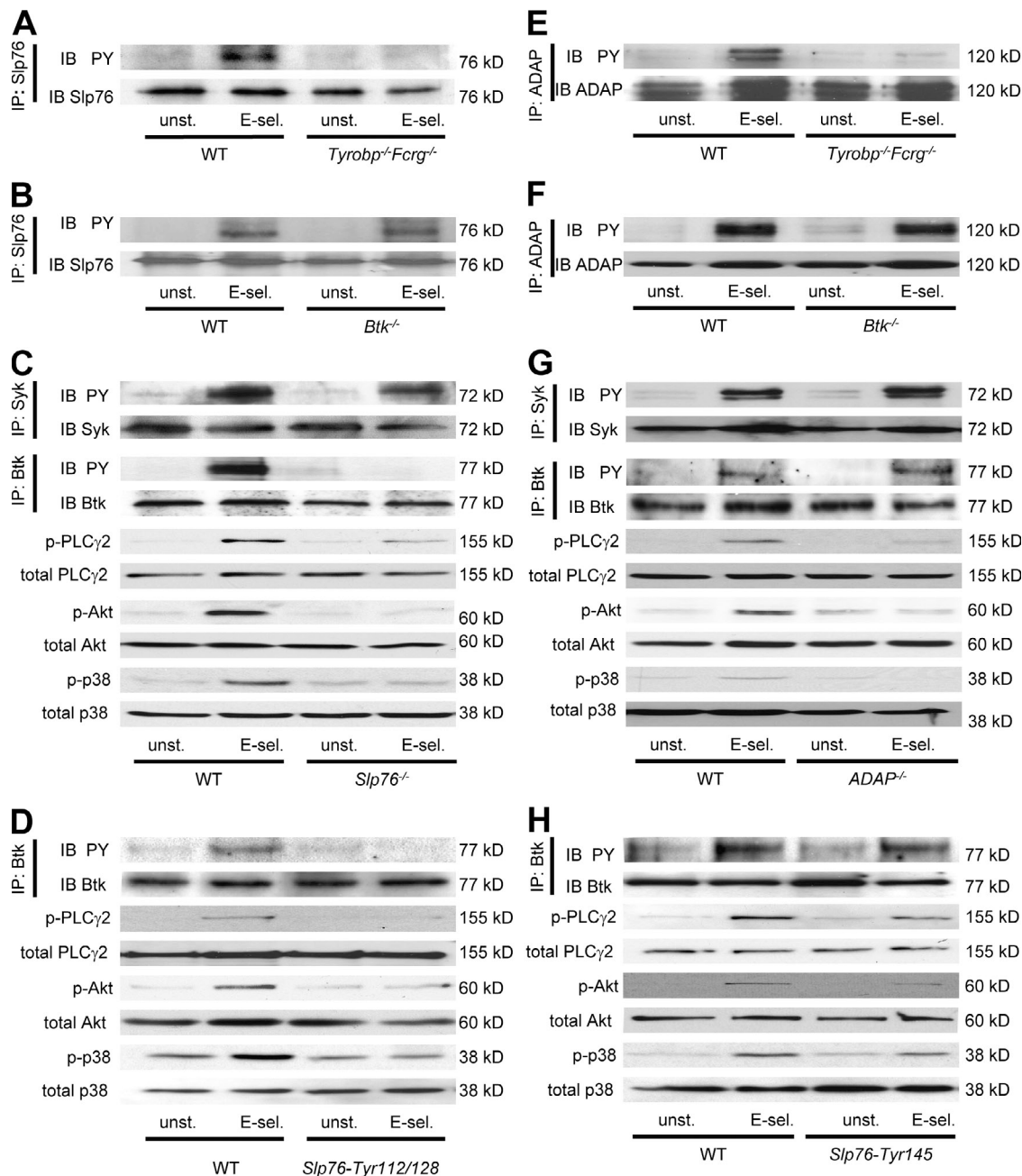
Figure 6. SLP-76 is required for the activation of Btk, PLCγ2, PI3Kγ, and p38 MAPK after E–selectin engagement. BM-derived neutrophils were plated on uncoated (unstimulated) or E-selectin–coated wells for 10 min, and then lysates were prepared. (A and B) Lysates of WT, Tyrobp$^{-/-}$Fcrg$^{-/-}$ (A; n = 3), and Btk$^{-/-}$ (B; n = 3) were immunoprecipitated (IP) with a SLP-76 antibody followed by immunoblotting (IB) with a general phosphotyrosine (PY; 4G10) antibody or total SLP-76 antibody. (C) Lysates of WT and Slp76$^{-/-}$ neutrophils were immunoprecipitated with an Syk (n = 3) or Btk antibody (n = 3) followed by immunoblotting with a general phosphotyrosine (4G10) antibody, total Syk antibody (n = 3), or total Btk antibody (n = 3). Lysates were immunoblotted with antibody to phosphorylated PLCγ2 (p-PLCγ2 [Tyr1217]; n = 3), total PLCγ2 (n = 3), phosphorylated Akt (n = 3), total Akt (n = 3), phosphorylated p38 MAPK (p-p38), or total p38 MAPK (n = 3). (D) Lysates of WT and Slp76$^{Y112/128}$ neutrophils were immunoprecipitated with Btk antibody (n = 3) followed by immunoblotting with a general phosphotyrosine (4G10) antibody or total Btk antibody (n = 3). Lysates were immunoblotted with antibody to phosphorylated PLCγ2 (Tyr1217; n = 3), total PLCγ2 (n = 3), phosphorylated Akt (n = 3), total Akt (n = 3), phosphorylated p38 MAPK, or total p38 MAPK (n = 3). (E and F) Lysates of WT, Tyrobp$^{-/-}$Fcrg$^{-/-}$ (E; n = 3), and Btk$^{-/-}$ neutrophils (F; n = 3) were immunoprecipitated with an ADAP antibody followed by immunoblotting with a general phosphotyrosine (4G10) antibody or total ADAP antibody. (G) Lysates of WT and ADAP$^{-/-}$ neutrophils were immunoprecipitated with an Syk (n = 3) or Btk antibody (n = 3) followed by immunoblotting with a general phosphotyrosine (4G10) antibody, total Syk antibody (n = 3), or total Btk antibody (n = 3). Lysates were immunoblotted with antibody to phosphorylated PLCγ2 (Tyr1217; n = 3), total PLCγ2 (n = 3), phosphorylated Akt (n = 3), total Akt (n = 3), phosphorylated p38 MAPK, or total p38 MAPK (n = 3). (H) Lysates of WT and Slp76^{Y145} neutrophils were immunoprecipitated with Btk antibody followed by immunoblotting with a general phosphotyrosine antibody (4G10). Lysates were also immunoblotted with antibody to phosphorylated PLCγ2 (Tyr1217; n = 3), total PLCγ2 (n = 3), phosphorylated Akt (n = 3), total Akt (n = 3), phosphorylated p38 MAPK, or total p38 MAPK (n = 3).

Blocking

Blocking this pathway completely abolishes integrin affinity and avidity regulation.

AKI is characterized by a strong recruitment of neutrophils into kidneys (Bonventre and Weinberg, 2003; Singbartl and Ley, 2004). Clinically, AKI has a poor prognosis and high mortality worldwide as there is no efficient pharmacologic therapy available that supports intensive care measures (Murugan and Kellum, 2011). A potential preventive effect of E-selectin blockade has been suggested for myocardial (Altavilla et al., 1994) and renal (Singbartl and Ley, 2000) ischemia-reperfusion–induced injury. Our study is the first to demonstrate a distinct role for E-selectin–mediated signaling in neutrophils in ischemia-reperfusion–induced organ failure. E-selectin induces slow leukocyte rolling via integrin activation (Zarbock et al., 2007a; Kuwano et al., 2010; Yago et al., 2010). This is necessary for subsequent leukocyte arrest. As shown in this study, SLP-76 and ADAP are essential molecules in this signaling pathway. It is well documented that leukocytes are recruited into the inflamed renal tissue and contribute to tissue injury and impairment of kidney function after renal IRI (Bonventre and Weinberg, 2003; Singbartl and Ley, 2004). Neutrophil depletion before induction of renal IRI abolishes the development of AKI (Singbartl et al., 2000). These data clearly demonstrate that neutrophil recruitment into the renal tissue is involved in the pathogenesis of AKI. As E-selectin–induced integrin activation and leukocyte rolling contribute to leukocyte recruitment into inflamed tissue (also into the inflamed kidney, as directly demonstrated by intravital microscopy), blocking of this pathway reduces the amount of neutrophils in the injured kidneys and therefore attenuates the severity of the AKI. Therefore, altering neutrophil recruitment through modulation of the E-selectin–mediated signaling pathway in neutrophils may constitute a valuable therapeutic avenue in conditions of acute inflammation including AKI in humans.

In this study, we show, for the first time, the physiological relevance of the E-selectin–mediated signaling pathway in a clinically relevant disease model. The disadvantage of the animal models used in the past to study E-selectin–mediated signaling was that $G\alpha_i$ signaling had to be blocked. In thioglycollate-induced peritonitis, neutrophil recruitment was not reduced after blocking E-selectin–mediated signaling but was partially inhibited after PTx treatment in WT mice (Smith et al., 2004; Zarbock et al., 2007a, 2008; Mueller et al., 2010; Yago et al., 2010). Blocking both pathways completely blocked neutrophil recruitment, suggesting that E-selectin– and $G\alpha_i$-mediated adhesion mechanisms are overlapping in this model. E-selectin–mediated and $G\alpha_i$ signaling have a redundant role in TNF-induced neutrophil adhesion and recruitment in the postcapillary venules of the cremaster muscle (Smith et al., 2004; Mueller et al., 2010). In contrast to these models, blocking of E-selectin–mediated signaling in the presence of $G\alpha_i$ signaling blocked neutrophil recruitment into the kidney and improved kidney function after ischemia-reperfusion induced AKI, suggesting that the E-selectin–mediated signaling pathway is a major pathway in this disease model.

To our knowledge, this is the first in vivo study that investigates the role of ADAP in neutrophil activation and recruitment. Structure–function analysis of the ADAP/SLP-76 signaling module revealed that a mutation within SLP-76 that impedes the binding between the two molecules also strongly attenuated integrin activation and abolished slow leukocyte rolling. Furthermore, we demonstrate that ADAP is involved in E-selectin–mediated integrin activation and slow leukocyte rolling, which promotes ischemia-reperfusion–induced AKI. SLP-76 but not ADAP is required for Btk activation as Btk phosphorylation is present in $ADAP^{-/-}$ neutrophils after E-selectin engagement. However, activation of the PLCγ2- and PI3Kγ-dependent pathways is impaired in the absence of ADAP, suggesting that both molecules, Btk and ADAP, are required for the activation of PLCγ2 and PI3Kγ. In contrast to the E-selectin–mediated signaling pathway, it has been shown that the presence of ADAP is not required for PLCγ1 and Rap1 activation, but rather for recruitment of this GTPase to the plasma membrane in response to TCR triggering (Griffiths et al., 2001; Peterson et al., 2001; Kliche et al., 2006; Ménasché et al., 2007). However, in the E-selectin–mediated signaling pathway, Rap1 is located downstream of PLCγ2 (Stadtmann et al., 2011), suggesting that both pathways use the same molecules but the sequence of the molecules is different.

In addition to the E-selectin–mediated leukocyte recruitment defect seen in $Slp76^{-/-}$ mice, the abnormal vascular and lymphatic architecture, the platelet defect, and the high output cardiac failure in $Slp76^{-/-}$ mice (Abtahian et al., 2003) may affect the development of ischemia-reperfusion–induced AKI. As Slp76^{Y145} mice have a normal vascular and lymphatic architecture and show the same number of neutrophils in the kidney and plasma creatinine levels as $Slp76^{-/-}$ mice after ischemia-reperfusion–induced AKI, it is unlikely that the abnormal vascular and lymphatic architecture in $Slp76^{-/-}$ mice affects the development of AKI. But it is still possible that the platelet defect seen in $Slp76^{-/-}$ mice and $Slp76^{Y145}$ mice (Clements et al., 1999; Bezman et al., 2008) may affect the development of AKI after IRI. However, the intravital microscopy experiments of the kidneys with the reconstituted knockout leukocytes in WT mice demonstrated that the absence of SLP-76 and ADAP in leukocytes abolishes E-selectin–mediated slow rolling and adhesion after renal IRI.

Based on different studies using cell lines (Koretzky and Myung, 2001), a model was established postulating that Y112 and Y128 are both required for the association of SLP-76 with Vav and/or Nck, whereas Tec family protein tyrosine kinases bind to Y145. As we and other groups demonstrated that Btk is involved in E-selectin–mediated slow rolling, we predicted that neutrophils isolated from Y145F mice would show abolished slow leukocyte rolling on E-selectin and ICAM-1. Therefore, we were surprised to find no evidence of abrogated E-selectin–mediated slow leukocyte rolling and phosphorylation of downstream signaling molecules in Y145F mice. Therefore, we investigated whether neutrophils from Y112/128F mice have reduced E-selectin–mediated slow

leukocyte rolling in vitro and in vivo. Interestingly, neutrophils from Y112/128F mice showed an abolished E-selectin–mediated downstream signaling and slow leukocyte rolling. Furthermore, Y112/128F mice showed a reduced number of neutrophils in the inflamed kidney and a diminished creatinine rise after renal IRI. As Btk does not directly interact with the tyrosines in position 112 and 128, the data presented in this study suggest that additional molecules, which can directly interact with SLP-76 and Btk, are involved in Btk activation after E-selectin engagement. Possible molecules that could link SLP-76 to Btk are members of the Vav family, as they interact with Tec family kinases and Y112 and Y128 in SLP-76. Vav molecules are involved in Tec family kinases' activation in thymocytes upon TCR engagement (Koretzky et al., 2006). Another possibility is that the SH3 and SH2 domains in Btk interact cooperatively with phosphorylated SLP-76 after E-selectin engagement. In contrast to our data, Y145 is critical for TCR–dependent Itk (IL-2–inducible T cell kinase)-associated functions in thymocytes and glycoprotein VI–induced activation of Btk in platelets (Bezman et al., 2008). Furthermore, data generated with primary myeloid cells from $Slp76^{Y145}$ mice demonstrate a reduced FcR–induced PLCγ phosphorylation in mast cells and diminished Ca^{2+} flux in mast cells and neutrophils, suggesting that Y145 is required for full FcR–induced Btk activation (Lenox et al., 2009). Furthermore, this study convincingly demonstrated that $Slp76^{Y145}$ mice were completely protected from serum–induced arthritis compared with WT and $Slp76^{Y112/128}$ mice (Lenox et al., 2009). However, our data are in line with a recently published study showing that Tec kinases bind to Y145F mutant SLP-76 in primary murine thymocytes (Jordan et al., 2008) and that the mutation of Y112 and Y128 ablated nearly all detectable SLP-76 phosphorylation after TCR stimulation. Clearly further experiments are required to solve this puzzle.

GPCR– and TCR–triggered signaling pathways modulate integrin affinity and avidity (Hogg et al., 2011; Kempf et al., 2011). It has been shown that E-selectin–mediated signaling induces the extended conformation of LFA-1 in neutrophils (Kuwano et al., 2010). In this study, we show that E-selectin engagement affects integrin activation by modulating conformational change and clustering (Fig. 4). Blocking E-selectin–mediated signaling by using gene-deficient neutrophils or specific pharmacological inhibitors abolished integrin activation (affinity and avidity). These data raise the question of whether a physiological mediator exists that can only regulate one modality (affinity or avidity) without affecting the other modality. Other in vitro and in vivo studies already demonstrated that E-selectin engagement induced the polarization of different adhesion molecules (Simon et al., 2000; Green et al., 2004; Hidalgo et al., 2007; Stadtmann et al., 2011), but LFA-1 clustering was not investigated in these studies. Further studies have to address the question of whether the increased LFA-1 avidity after E-selectin binding participates in regulating the rolling velocity or converting the rolling to arrest.

These data demonstrate the physiological relevance of the E-selectin–mediated signaling pathway in vivo. The new mechanistic insights we provide in this study suggest that SLP-76 and ADAP may be therapeutic targets for anti-inflammatory therapy.

MATERIALS AND METHODS

Animals and BM chimeras. 8–12-wk-old C57BL/6 (JANVIER), $ADAP^{-/-}$ (Peterson et al., 2001), $Syk^{-/-}$ (Mueller et al., 2010), $Tyrobp^{-/-}Fcrg^{-/-}$ (Zarbock et al., 2008), $Pik3cg^{-/-}$ (Mueller et al., 2010), $Plcg2^{-/-}$ (Mueller et al., 2010), $Slp76^{-/-}$ (Clements et al., 1999), Slp76^{Y112/128} (Jordan et al., 2008), Slp76^{Y145} (Jordan et al., 2008), and $Btk^{-/-}$ mice (The Jackson Laboratory) were housed in a special pathogen–free facility. The Animal Care and Use Committees of the University of Münster approved all animal experiments.

Chimeric mice were generated by performing BM transplantation as described previously (Mueller et al., 2010). In brief, BM cells were isolated from gene–deficient mice ($ADAP^{-/-}$, $Slp76^{-/-}$, and Slp76^{Y112/128} or Slp76^{Y145} mice). These cells were injected i.v. (2×10^6/recipient) into lethally irradiated WT mice (9.5 Gy). Experiments were performed 6–8 wk after BM transplantation.

Reagents. If not stated otherwise, all reagents were obtained from Sigma-Aldrich.

Cell lines and constructs. HL-60 cells were transfected with the shRNA-expressing constructs pCMS4-SHC (control), pCMS4-SHSlp76, and pCMS4-SHADAP (Horn et al., 2009) by using the Nucleofection Amaxa kit V (Lonza) according to the manufacturer's instructions. The transfection rate was determined by flow cytometry, and the down-regulation of the protein was assessed by Western blot. Furthermore, the retroviral constructs pMIGR1-Slp76 and pMIGR1-Slp76R448K were used (Baker et al., 2009).

Hematopoietic stem cell isolation and retroviral transduction. Retroviral supernatants were generated by transfecting a packaging cell line with the respective constructs using Nanofectin (PAA). Supernatants were collected and used for infection of hematopoietic stem and progenitor cells as described previously (Mócsai et al., 2006). In brief, BM cells were isolated from gene–deficient mice ($Slp76^{-/-}$) and were subjected to lineage depletion by using a lineage cell depletion kit (Miltenyi Biotec) according to the manufacturer's protocol. Purified hematopoietic stem and progenitor cells were preincubated overnight in BM stimulation medium (DME [Invitrogen]), 20% fetal calf serum supplemented with 10 ng/ml of murine IL-3, 5 ng/ml of murine IL-6, and 50 ng/ml of murine stem cell factor (all cytokines from PeproTech). RetroNectin–coated culture dishes (50 µg/ml; Takara Bio Inc.) were used to concentrate the viral particles. The prestimulated BM was seeded for overnight incubation on these plates with a density of 2×10^6/plate in 3 ml BM stimulation medium. After 2 d of transduction, efficiency was measured by flow cytometry. BM transplantation was performed as described previously (Zarbock et al., 2008).

Autoperfused flow chamber. Autoperfused flow chamber experiments were performed as described previously (Zarbock et al., 2007a, 2008; Mueller et al., 2010). In brief, rectangular glass capillaries were coated with 2.5 µg/ml E-selectin alone or in combination with 2 µg/ml ICAM-1 (R&D Systems) for 2 h and then blocked for 1 h using casein (Thermo Fisher Scientific). To control the wall shear stress in the capillary, a PE-50 tubing (BD) was connected to one side of the capillary. The other side of the chamber was connected to a PE-10 tubing and inserted into a mouse carotid artery. Leukocyte rolling was recorded for 1 min using an SW40/0.75 objective and a digital camera (Sensicam QE; Cooke Corporation).

Adhesion flow chamber. Adhesion flow chamber experiments were performed as described previously (Kuwano et al., 2010). In brief, protein G–precoated glass capillaries were coated with 6.6 µg/ml E-selectin and 25 µg/ml IgG1 or 25 µg/ml KIM127 for 1 h and blocked with casein. HL-60 cells were resuspended in PBS containing 1 mM $MgCl_2$ and $CaCl_2$ with a density of 5×10^6/ml living cells. The flow chamber was perfused

with the cell suspension for 2 min and washed with PBS (1 mM MgCl₂/CaCl₂) for 1 min. In representative images, the number of cells per field of view was determined. In some experiments, whole human blood was incubated for 30 min at room temperature with inhibitors against Btk (25 µM, LFM-A13), PLC (10 µM, U73122), PI3Kγ (0.5 µM, 528106; EMD), or DMSO.

Peritonitis model. The recruitment of leukocytes into the inflamed peritoneum was induced by using thioglycollate as described previously (Zarbock et al., 2008; Mueller et al., 2010). In brief, 1 ml of sterile thioglycollate (3%; Sigma-Aldrich) was injected intraperitoneally. Some mice received tail vein injections of 4 µg PTx 2 h before thioglycollate injection. 8 h after injection, mice were euthanized, and the peritoneum was rinsed with 10 ml PBS (containing 5 mM EDTA and 10 U/ml heparin). The total number of leukocytes was counted, and the percentage of neutrophils was determined by flow cytometry (FACSCanto; BD) based on the expression of CD45 (clone 30-F11), GR-1 (clone RB6-8C5), and 7/4 (clone 7/4; both BD).

Selectin engagement assay. BM-derived neutrophils were suspended in PBS (1 mM CaCl₂/MgCl₂) and stimulated on E-selectin–coated dishes at 65 rpm for 10 min as described previously (Zarbock et al., 2008; Mueller et al., 2010; Stadtmann et al., 2011). Neutrophils were lysed with RIPA buffer. Lysates were boiled with sample buffer or incubated with Sepharose A/G beads (Santa Cruz Biotechnology, Inc.) and anti-Fyb (Millipore), anti-Slp76, anti-Btk, or anti-Syk (Santa Cruz Biotechnology, Inc.) antibody for 4 h on ice. Beads were washed four times, and bound proteins were eluted by adding boiling sample buffer.

Cell lysates and immunoprecipitates were run on 10% SDS-PAGE and immunoblotted using antibodies against phosphotyrosine (4G10; Millipore), p38 MAPK, phospho-p38 MAPK, Akt, phospho-Akt (Thr308), PLCγ2, phospho-PLCγ2 (Tyr1217), and Slp76 (all from Cell Signaling Technology), and Btk, Fyb, or Syk (Santa Cruz Biotechnology, Inc.). Immunoblots were developed using an ECL system (GE Healthcare).

Intravital microscopy. To induce inflammation, mice received an intrascrotal injection of 500 ng TNF (R&D Systems) in 0.3 ml of saline 2 h before cremaster muscle exteriorization. Some animals also received tail vein injections of 4 µg PTx (Sigma-Aldrich) suspended in 0.3 ml of saline 5 min before TNF injection. Mice were anesthetized using intraperitoneal injection of 12.5 mg/kg xylazine (Tranqui Ved; Phoenix Scientific Inc.) and 125 mg/kg ketamine hydrochloride (Sanofi Winthrop Pharmaceuticals), and the cremaster muscle was prepared for intravital imaging as described previously (Zarbock et al., 2007a, 2008; Mueller et al., 2010; Stadtmann et al., 2011). Intravital microscopy was performed on an upright microscope (Axioskop; Carl Zeiss) with a 40× NA 0.75 saline immersion objective. Leukocyte rolling velocity and leukocyte arrest were determined by transillumination intravital microscopy, whereas leukocyte extravasation was investigated by reflected light oblique transillumination microscopy as described previously (Mueller et al., 2010; Stadtmann et al., 2011). Clustering of surface adhesion molecules (LFA-1) was performed as described previously (Stadtmann et al., 2011). Recorded images were analyzed using ImageJ (National Institutes of Health) and AxioVision (Carl Zeiss) software. Emigrated cells were determined in an area reaching out 75 µm to each side of a vessel over a distance of 100-µm vessel length (representing a 1.5×10^4–µm² tissue area). The microcirculation was recorded using a digital camera (Sensicam QE). Postcapillary venules with a diameter between 20 and 40 µm were investigated. Blood flow centerline velocity was measured using a dual photodiode sensor system (Circusoft Instrumentation), and centerline velocities were calculated as described previously (Zarbock et al., 2007a, 2008; Mueller et al., 2010; Stadtmann et al., 2011). In some experiments, ischemia of the cremaster muscle was achieved by tying off the supplying arteries with polyethylene-10 tubing and visually confirming that blood flow had ceased (Prorock et al., 2003).

RIR to induce acute renal failure. The RIR model has been described previously (Zarbock et al., 2007b). In brief, mice were anesthetized with intraperitoneal injections of ketamine and xylazine and were placed on a heating pad to maintain body temperature. In animals undergoing RIR, both renal pedicles were clamped off for 32 min with hemostatic microclips. Kidneys were inspected for immediate color change, indicating successful clamping. After clamp removal, kidneys were checked for a change in color within 3 min to ensure reperfusion. In animals subjected to sham operation, the surgical procedure was identical except that no clamps were applied. Incisions were closed in two layers, and animals were allowed to recover. After 24 h, the mice were euthanized, blood samples were taken by heart puncture, and kidneys were harvested to determine the number of neutrophils in the kidney. Creatinine levels in the blood plasma were determined by using a creatinine assay (Diazyme) according to the manufacturer's protocol. Neutrophil recruitment into the kidneys was determined by using flow cytometry as previously described (Zarbock et al., 2007b).

In some experiments, intravital microscopy of small vessels in the cortex of the kidney was performed 4 h after sham operation or renal IRI. LysM-GFP⁺ mice were used to directly investigate leukocyte rolling and adhesion. In some experiments, blocking antibodies were used against E-selectin (9A9, 100 µg), LFA-1 (TIB-217, 30 µg), or Mac-1 (M1-70, 30 µg).

To investigate GFP-negative mice, WT mice that underwent RIR were injected with fluorescently labeled BM cells from WT, Slp76⁻/⁻, Slp76^Y145, Slp76^Y112/128, or ADAP⁻/⁻ mice 2 h before microscopy. Labeling with CMFDA cell tracker (Invitrogen) was performed according to the manufacturer's instructions. Microscopy was performed using an upright microscope (Axioskop) with a 20× NA 0.5 saline immersion objective. Hematoxylin and eosin (H&E) staining of paraffin-embedded organs was performed according to standard protocols.

Statistics. Statistical analysis was performed with SPSS software (version 14.0). Differences between the groups were evaluated by one-way analysis of variance, Student Newman–Keuls test, and Student's t test where appropriate. Data are presented as mean ± SEM, and $P < 0.05$ was considered statistically significant.

REFERENCES

Abtahian, F., A. Guerriero, E. Sebzda, M.M. Lu, R. Zhou, A. Mocsai, E.E. Myers, B. Huang, D.G. Jackson, V.A. Ferrari, et al. 2003. Regulation of blood and lymphatic vascular separation by signaling proteins SLP-76 and Syk. *Science*. 299:247–251. http://dx.doi.org/10.1126/science.1079477

Altavilla, D., F. Squadrito, M. Ioculano, P. Canale, G.M. Campo, B. Zingarelli, and A.P. Caputi. 1994. E-selectin in the pathogenesis of experimental myocardial ischemia-reperfusion injury. *Eur. J. Pharmacol*. 270:45–51.

Baker, R.G., C.J. Hsu, D. Lee, M.S. Jordan, J.S. Maltzman, D.A. Hammer, T. Baumgart, and G.A. Koretzky. 2009. The adapter protein SLP-76 mediates "outside-in" integrin signaling and function in T cells. *Mol. Cell. Biol*. 29:5578–5589. http://dx.doi.org/10.1128/MCB.00283-09

Bezman, N.A., L. Lian, C.S. Abrams, L.F. Brass, M.L. Kahn, M.S. Jordan, and G.A. Koretzky. 2008. Requirements of SLP76 tyrosines in ITAM and integrin receptor signaling and function in platelet in vivo. *J. Exp. Med*. 205:1775–1788. http://dx.doi.org/10.1084/jem.20080240

Bonventre, J.V., and J.M. Weinberg. 2003. Recent advances in the pathophysiology of ischemic acute renal failure. *J. Am. Soc. Nephrol*. 14:2199–2210. http://dx.doi.org/10.1097/01.ASN.0000079785.13922.F6

Bubeck Wardenburg, J., C. Fu, J.K. Jackman, H. Flotow, S.E. Wilkinson, D.H. Williams, R. Johnson, G. Kong, A.C. Chan, and P.R. Findell.

1996. Phosphorylation of SLP-76 by the ZAP-70 protein-tyrosine kinase is required for T-cell receptor function. *J. Biol. Chem.* 271:19641–19644. http://dx.doi.org/10.1074/jbc.271.33.19641

Bubeck Wardenburg, J., R. Pappu, J.Y. Bu, B. Mayer, J. Chernoff, D. Straus, and A.C. Chan. 1998. Regulation of PAK activation and the T cell cytoskeleton by the linker protein SLP-76. *Immunity.* 9:607–616. http://dx.doi.org/10.1016/S1074-7613(00)80658-5

Clemens, R.A., L.E. Lenox, T. Kambayashi, N. Bezman, J.S. Maltzman, K.E. Nichols, and G.A. Koretzky. 2007. Loss of SLP-76 expression within myeloid cells confers resistance to neutrophil-mediated tissue damage while maintaining effective bacterial killing. *J. Immunol.* 178:4606–4614.

Clements, J.L., J.R. Lee, B. Gross, B. Yang, J.D. Olson, A. Sandra, S.P. Watson, S.R. Lentz, and G.A. Koretzky. 1999. Fetal hemorrhage and platelet dysfunction in SLP-76-deficient mice. *J. Clin. Invest.* 103:19–25. http://dx.doi.org/10.1172/JCI5317

da Silva, A.J., Z. Li, C. de Vera, E. Canto, P. Findell, and C.E. Rudd. 1997. Cloning of a novel T-cell protein FYB that binds FYN and SH2-domain-containing leukocyte protein 76 and modulates interleukin 2 production. *Proc. Natl. Acad. Sci. USA.* 94:7493–7498. http://dx.doi.org/10.1073/pnas.94.14.7493

Eltzschig, H.K., and P. Carmeliet. 2011. Hypoxia and inflammation. *N. Engl. J. Med.* 364:656–665. http://dx.doi.org/10.1056/NEJMra0910283

Fang, N., D.G. Motto, S.E. Ross, and G.A. Koretzky. 1996. Tyrosines 113, 128, and 145 of SLP-76 are required for optimal augmentation of NFAT promoter activity. *J. Immunol.* 157:3769–3773.

Faust, N., F. Varas, L.M. Kelly, S. Heck, and T. Graf. 2000. Insertion of enhanced green fluorescent protein into the lysozyme gene creates mice with green fluorescent granulocytes and macrophages. *Blood.* 96:719–726.

Geng, L., M. Raab, and C.E. Rudd. 1999. Cutting edge: SLP-76 cooperativity with FYB/FYN-T in the Up-regulation of TCR-driven IL-2 transcription requires SLP-76 binding to FYB at Tyr595 and Tyr651. *J. Immunol.* 163:5753–5757.

Geng, L., S. Pfister, S.K. Kraeft, and C.E. Rudd. 2001. Adaptor FYB (Fyn-binding protein) regulates integrin-mediated adhesion and mediator release: Differential involvement of the FYB SH3 domain. *Proc. Natl. Acad. Sci. USA.* 98:11527–11532. http://dx.doi.org/10.1073/pnas.191378198

Green, C.E., D.N. Pearson, R.T. Camphausen, D.E. Staunton, and S.I. Simon. 2004. Shear-dependent capping of L-selectin and P-selectin glycoprotein ligand 1 by E-selectin signals activation of high-avidity beta2-integrin on neutrophils. *J. Immunol.* 172:7780–7790.

Griffiths, E.K., C. Krawczyk, Y.Y. Kong, M. Raab, S.J. Hyduk, D. Bouchard, V.S. Chan, I. Kozieradzki, A.J. Oliveira-Dos-Santos, A. Wakeham, et al. 2001. Positive regulation of T cell activation and integrin adhesion by the adapter Fyb/Slap. *Science.* 293:2260–2263. http://dx.doi.org/10.1126/science.1063397

Gross, B.S., J.R. Lee, J.L. Clements, M. Turner, V.L. Tybulewicz, P.R. Findell, G.A. Koretzky, and S.P. Watson. 1999. Tyrosine phosphorylation of SLP-76 is downstream of Syk following stimulation of the collagen receptor in platelets. *J. Biol. Chem.* 274:5963–5971. http://dx.doi.org/10.1074/jbc.274.9.5963

Heuer, K., A. Arbuzova, H. Strauss, M. Kofler, and C. Freund. 2005. The helically extended SH3 domain of the T cell adaptor protein ADAP is a novel lipid interaction domain. *J. Mol. Biol.* 348:1025–1035. http://dx.doi.org/10.1016/j.jmb.2005.02.069

Hidalgo, A., A.J. Peired, M.K. Wild, D. Vestweber, and P.S. Frenette. 2007. Complete identification of E-selectin ligands on neutrophils reveals distinct functions of PSGL-1, ESL-1, and CD44. *Immunity.* 26:477–489. http://dx.doi.org/10.1016/j.immuni.2007.03.011

Hogg, N., I. Patzak, and F. Willenbrock. 2011. The insider's guide to leukocyte integrin signalling and function. *Nat. Rev. Immunol.* 11:416–426. http://dx.doi.org/10.1038/nri2986

Horn, J., X. Wang, P. Reichardt, T.E. Stradal, N. Warnecke, L. Simeoni, M. Gunzer, D. Yablonski, B. Schraven, and S. Kliche. 2009. Src homology 2-domain containing leukocyte-specific phosphoprotein of 76 kDa is mandatory for TCR-mediated inside-out signaling, but dispensable for CXCR4-mediated LFA-1 activation, adhesion, and migration of T cells. *J. Immunol.* 183:5756–5767. http://dx.doi.org/10.4049/jimmunol.0900649

Jordan, M.S., A.L. Singer, and G.A. Koretzky. 2003. Adaptors as central mediators of signal transduction in immune cells. *Nat. Immunol.* 4:110–116. http://dx.doi.org/10.1038/ni0203-110

Jordan, M.S., J. Sadler, J.E. Austin, L.D. Finkelstein, A.L. Singer, P.L. Schwartzberg, and G.A. Koretzky. 2006. Functional hierarchy of the N-terminal tyrosines of SLP-76. *J. Immunol.* 176:2430–2438.

Jordan, M.S., J.E. Smith, J.C. Burns, J.E. Austin, K.E. Nichols, A.C. Aschenbrenner, and G.A. Koretzky. 2008. Complementation in trans of altered thymocyte development in mice expressing mutant forms of the adaptor molecule SLP76. *Immunity.* 28:359–369. http://dx.doi.org/10.1016/j.immuni.2008.01.010

Judd, B.A., P.S. Myung, L. Leng, A. Obergfell, W.S. Pear, S.J. Shattil, and G.A. Koretzky. 2000. Hematopoietic reconstitution of SLP-76 corrects hemostasis and platelet signaling through alpha IIb beta 3 and collagen receptors. *Proc. Natl. Acad. Sci. USA.* 97:12056–12061. http://dx.doi.org/10.1073/pnas.97.22.12056

Judd, B.A., P.S. Myung, A. Obergfell, E.E. Myers, A.M. Cheng, S.P. Watson, W.S. Pear, D. Allman, S.J. Shattil, and G.A. Koretzky. 2002. Differential requirement for LAT and SLP-76 in GPVI versus T cell receptor signaling. *J. Exp. Med.* 195:705–717. http://dx.doi.org/10.1084/jem.20011583

Kasirer-Friede, A., B. Moran, J. Nagrampa-Orje, K. Swanson, Z.M. Ruggeri, B. Schraven, B.G. Neel, G. Koretzky, and S.J. Shattil. 2007. ADAP is required for normal alphaIIbbeta3 activation by VWF/GP Ib-IX-V and other agonists. *Blood.* 109:1018–1025. http://dx.doi.org/10.1182/blood-2006-05-022301

Kempf, T., A. Zarbock, C. Widera, S. Butz, A. Stadtmann, J. Rossaint, M. Bolomini-Vittori, M. Korf-Klingebiel, L.C. Napp, B. Hansen, et al. 2011. GDF-15 is an inhibitor of leukocyte integrin activation required for survival after myocardial infarction in mice. *Nat. Med.* 17:581–588. http://dx.doi.org/10.1038/nm.2354

Kettner, A., V. Pivniouk, L. Kumar, H. Falet, J.S. Lee, R. Mulligan, and R.S. Geha. 2003. Structural requirements of SLP-76 in signaling via the high-affinity immunoglobulin E receptor (Fc epsilon RI) in mast cells. *Mol. Cell. Biol.* 23:2395–2406. http://dx.doi.org/10.1128/MCB.23.7.2395-2406.2003

Kliche, S., D. Breitling, M. Togni, R. Pusch, K. Heuer, X. Wang, C. Freund, A. Kasirer-Friede, G. Menasche, G.A. Koretzky, and B. Schraven. 2006. The ADAP/SKAP55 signaling module regulates T-cell receptor-mediated integrin activation through plasma membrane targeting of Rap1. *Mol. Cell. Biol.* 26:7130–7144. http://dx.doi.org/10.1128/MCB.00331-06

Koretzky, G.A., and P.S. Myung. 2001. Positive and negative regulation of T-cell activation by adaptor proteins. *Nat. Rev. Immunol.* 1:95–107. http://dx.doi.org/10.1038/35100523

Koretzky, G.A., F. Abtahian, and M.A. Silverman. 2006. SLP76 and SLP65: complex regulation of signalling in lymphocytes and beyond. *Nat. Rev. Immunol.* 6:67–78. http://dx.doi.org/10.1038/nri1750

Krause, M., A.S. Sechi, M. Konradt, D. Monner, F.B. Gertler, and J. Wehland. 2000. Fyn-binding protein (Fyb)/SLP-76–associated protein (SLAP), Ena/vasodilator-stimulated phosphoprotein (VASP) proteins and the Arp2/3 complex link T cell receptor (TCR) signaling to the actin cytoskeleton. *J. Cell Biol.* 149:181–194. http://dx.doi.org/10.1083/jcb.149.1.181

Kuwano, Y., O. Spelten, H. Zhang, K. Ley, and A. Zarbock. 2010. Rolling on E- or P-selectin induces the extended but not high-affinity conformation of LFA-1 in neutrophils. *Blood.* 116:617–624. http://dx.doi.org/10.1182/blood-2010-01-266122

Lenox, L.E., T. Kambayashi, M. Okumura, C. Prieto, K. Sauer, R.M. Bunte, M.S. Jordan, G.A. Koretzky, and K.E. Nichols. 2009. Mutation of tyrosine 145 of lymphocyte cytosolic protein 2 protects mice from anaphylaxis and arthritis. *J. Allergy Clin. Immunol.* 124:1088–1098. http://dx.doi.org/10.1016/j.jaci.2009.08.038

Ley, K., C. Laudanna, M.I. Cybulsky, and S. Nourshargh. 2007. Getting to the site of inflammation: the leukocyte adhesion cascade updated. *Nat. Rev. Immunol.* 7:678–689. http://dx.doi.org/10.1038/nri2156

Ménasché, G., S. Kliche, E.J. Chen, T.E. Stradal, B. Schraven, and G. Koretzky. 2007. RIAM links the ADAP/SKAP-55 signaling module to Rap1, facilitating T-cell-receptor-mediated integrin activation. *Mol. Cell. Biol.* 27:4070–4081. http://dx.doi.org/10.1128/MCB.02011-06

Miner, J.J., L. Xia, T. Yago, J. Kappelmayer, Z. Liu, A.G. Klopocki, B. Shao, J.M. McDaniel, H. Setiadi, D.W. Schmidtke, and R.P. McEver. 2008. Separable requirements for cytoplasmic domain of PSGL-1 in leukocyte rolling and signaling under flow. *Blood*. 112:2035–2045. http://dx.doi.org/10.1182/blood-2008-04-149468

Mócsai, A., C.L. Abram, Z. Jakus, Y. Hu, L.L. Lanier, and C.A. Lowell. 2006. Integrin signaling in neutrophils and macrophages uses adaptors containing immunoreceptor tyrosine-based activation motifs. *Nat. Immunol*. 7:1326–1333. http://dx.doi.org/10.1038/ni1407

Motto, D.G., S.E. Ross, J. Wu, L.R. Hendricks-Taylor, and G.A. Koretzky. 1996. Implication of the GRB2-associated phosphoprotein SLP-76 in T cell receptor-mediated interleukin 2 production. *J. Exp. Med*. 183:1937–1943. http://dx.doi.org/10.1084/jem.183.4.1937

Mueller, H., A. Stadtmann, H. Van Aken, E. Hirsch, D. Wang, K. Ley, and A. Zarbock. 2010. Tyrosine kinase Btk regulates E-selectin–mediated integrin activation and neutrophil recruitment by controlling phospholipase C (PLC) gamma2 and PI3Kgamma pathways. *Blood*. 115:3118–3127. http://dx.doi.org/10.1182/blood-2009-11-254185

Murugan, R., and J.A. Kellum. 2011. Acute kidney injury: what's the prognosis? *Nat. Rev. Nephrol*. 7:209–217. http://dx.doi.org/10.1038/nrneph.2011.13

Musci, M.A., L.R. Hendricks-Taylor, D.G. Motto, M. Paskind, J. Kamens, C.W. Turck, and G.A. Koretzky. 1997. Molecular cloning of SLAP-130, an SLP-76-associated substrate of the T cell antigen receptor-stimulated protein tyrosine kinases. *J. Biol. Chem*. 272:11674–11677. http://dx.doi.org/10.1074/jbc.272.18.11674

Myung, P.S., G.S. Derimanov, M.S. Jordan, J.A. Punt, Q.H. Liu, B.A. Judd, E.E. Meyers, C.D. Sigmund, B.D. Freedman, and G.A. Koretzky. 2001. Differential requirement for SLP-76 domains in T cell development and function. *Immunity*. 15:1011–1026. http://dx.doi.org/10.1016/S1074-7613(01)00253-9

Nathan, C. 2006. Neutrophils and immunity: challenges and opportunities. *Nat. Rev. Immunol*. 6:173–182. http://dx.doi.org/10.1038/nri1785

Newbrough, S.A., A. Mocsai, R.A. Clemens, J.N. Wu, M.A. Silverman, A.L. Singer, C.A. Lowell, and G.A. Koretzky. 2003. SLP-76 regulates Fcgamma receptor and integrin signaling in neutrophils. *Immunity*. 19:761–769. http://dx.doi.org/10.1016/S1074-7613(03)00305-4

O'Shea, J.J., and P.J. Murray. 2008. Cytokine signaling modules in inflammatory responses. *Immunity*. 28:477–487. http://dx.doi.org/10.1016/j.immuni.2008.03.002

Peterson, E.J., M.L. Woods, S.A. Dmowski, G. Derimanov, M.S. Jordan, J.N. Wu, P.S. Myung, Q.H. Liu, J.T. Pribila, B.D. Freedman, et al. 2001. Coupling of the TCR to integrin activation by Slap-130/Fyb. *Science*. 293:2263–2265. http://dx.doi.org/10.1126/science.1063486

Prorock, A.J., A. Hafezi-Moghadam, V.E. Laubach, J.K. Liao, and K. Ley. 2003. Vascular protection by estrogen in ischemia-reperfusion injury requires endothelial nitric oxide synthase. *Am. J. Physiol. Heart Circ. Physiol*. 284:H133–H140.

Raab, M., A.J. da Silva, P.R. Findell, and C.E. Rudd. 1997. Regulation of Vav-SLP-76 binding by ZAP-70 and its relevance to TCR zeta/CD3 induction of interleukin-2. *Immunity*. 6:155–164. http://dx.doi.org/10.1016/S1074-7613(00)80422-7

Raab, M., H. Kang, A. da Silva, X. Zhu, and C.E. Rudd. 1999. FYN-T-FYB-SLP-76 interactions define a T-cell receptor zeta/CD3-mediated tyrosine phosphorylation pathway that up-regulates interleukin 2 transcription in T-cells. *J. Biol. Chem*. 274:21170–21179. http://dx.doi.org/10.1074/jbc.274.30.21170

Serhan, C.N., and J. Savill. 2005. Resolution of inflammation: the beginning programs the end. *Nat. Immunol*. 6:1191–1197. http://dx.doi.org/10.1038/ni1276

Simon, S.I., Y. Hu, D. Vestweber, and C.W. Smith. 2000. Neutrophil tethering on E-selectin activates beta 2 integrin binding to ICAM-1 through a mitogen-activated protein kinase signal transduction pathway. *J. Immunol*. 164:4348–4358.

Singbartl, K., and K. Ley. 2000. Protection from ischemia-reperfusion induced severe acute renal failure by blocking E-selectin. *Crit. Care Med*. 28:2507–2514. http://dx.doi.org/10.1097/00003246-200007000-00053

Singbartl, K., and K. Ley. 2004. Leukocyte recruitment and acute renal failure. *J. Mol. Med*. 82:91–101. http://dx.doi.org/10.1007/s00109-003-0498-8

Singbartl, K., S.A. Green, and K. Ley. 2000. Blocking P-selectin protects from ischemia/reperfusion–induced acute renal failure. *FASEB J*. 14:48–54.

Smith, M.L., T.S. Olson, and K. Ley. 2004. CXCR2- and E-selectin–induced neutrophil arrest during inflammation in vivo. *J. Exp. Med*. 200:935–939. http://dx.doi.org/10.1084/jem.20040424

Stadtmann, A., L. Brinkhaus, H. Mueller, J. Rossaint, M. Bolomini-Vittori, W. Bergmeier, H. Van Aken, D.D. Wagner, C. Laudanna, K. Ley, and A. Zarbock. 2011. Rap1a activation by CalDAG-GEFI and p38 MAPK is involved in E-selectin-dependent slow leukocyte rolling. *Eur. J. Immunol*. 41:2074–2085. http://dx.doi.org/10.1002/eji.201041196

Su, Y.W., Y. Zhang, J. Schweikert, G.A. Koretzky, M. Reth, and J. Wienands. 1999. Interaction of SLP adaptors with the SH2 domain of Tec family kinases. *Eur. J. Immunol*. 29:3702–3711. http://dx.doi.org/10.1002/(SICI)1521-4141(199911)29:11<3702::AID-IMMU3702>3.0.CO;2-R

Thadhani, R., M. Pascual, and J.V. Bonventre. 1996. Acute renal failure. *N. Engl. J. Med*. 334:1448–1460. http://dx.doi.org/10.1056/NEJM199605303342207

Urzainqui, A., J.M. Serrador, F. Viedma, M. Yáñez-Mó, A. Rodríguez, A.L. Corbí, J.L. Alonso-Lebrero, A. Luque, M. Deckert, J. Vázquez, and F. Sánchez-Madrid. 2002. ITAM-based interaction of ERM proteins with Syk mediates signaling by the leukocyte adhesion receptor PSGL-1. *Immunity*. 17:401–412. http://dx.doi.org/10.1016/S1074-7613(02)00420-X

Veale, M., M. Raab, Z. Li, A.J. da Silva, S.K. Kraeft, S. Weremowicz, C.C. Morton, and C.E. Rudd. 1999. Novel isoform of lymphoid adaptor FYN-T-binding protein (FYB-130) interacts with SLP-76 and up-regulates interleukin 2 production. *J. Biol. Chem*. 274:28427–28435. http://dx.doi.org/10.1074/jbc.274.40.28427

Wang, H., F.E. McCann, J.D. Gordan, X. Wu, M. Raab, T.H. Malik, D.M. Davis, and C.E. Rudd. 2004. ADAP–SLP-76 binding differentially regulates supramolecular activation cluster (SMAC) formation relative to T cell–APC conjugation. *J. Exp. Med*. 200:1063–1074. http://dx.doi.org/10.1084/jem.20040780

Wang, H.B., J.T. Wang, L. Zhang, Z.H. Geng, W.L. Xu, T. Xu, Y. Huo, X. Zhu, E.F. Plow, M. Chen, and J.G. Geng. 2007. P-selectin primes leukocyte integrin activation during inflammation. *Nat. Immunol*. 8:882–892. http://dx.doi.org/10.1038/ni1491

Yablonski, D., M.R. Kuhne, T. Kadlecek, and A. Weiss. 1998. Uncoupling of nonreceptor tyrosine kinases from PLC-gamma1 in an SLP-76-deficient T cell. *Science*. 281:413–416. http://dx.doi.org/10.1126/science.281.5375.413

Yago, T., B. Shao, J.J. Miner, L. Yao, A.G. Klopocki, K. Maeda, K.M. Coggeshall, and R.P. McEver. 2010. E-selectin engages PSGL-1 and CD44 through a common signaling pathway to induce integrin alphaL-beta2-mediated slow leukocyte rolling. *Blood*. 116:485–494. http://dx.doi.org/10.1182/blood-2009-12-259556

Zarbock, A., and K. Ley. 2008. Mechanisms and consequences of neutrophil interaction with the endothelium. *Am. J. Pathol*. 172:1–7. http://dx.doi.org/10.2353/ajpath.2008.070502

Zarbock, A., C.A. Lowell, and K. Ley. 2007a. Spleen tyrosine kinase Syk is necessary for E-selectin-induced alpha(L)beta(2) integrin-mediated rolling on intercellular adhesion molecule-1. *Immunity*. 26:773–783. http://dx.doi.org/10.1016/j.immuni.2007.04.011

Zarbock, A., M. Schmolke, S.G. Bockhorn, M. Scharte, K. Buschmann, K. Ley, and K. Singbartl. 2007b. The Duffy antigen receptor for chemokines in acute renal failure: A facilitator of renal chemokine presentation. *Crit. Care Med*. 35:2156–2163. http://dx.doi.org/10.1097/01.CCM.0000280570.82885.32

Zarbock, A., C.L. Abram, M. Hundt, A. Altman, C.A. Lowell, and K. Ley. 2008. PSGL-1 engagement by E-selectin signals through Src kinase Fgr and ITAM adapters DAP12 and FcRγ to induce slow leukocyte rolling. *J. Exp. Med*. 205:2339–2347. http://dx.doi.org/10.1084/jem.20072660